N75-26999

Copy No. 101

NASA CR-132670

A FUSELAGE/TANK STRUCTURE STUDY FOR ACTIVELY COOLED HYPERSONIC CRUISE VEHICLES

Structural Analysis

By Allen H. Baker

Prepared under Contract No. NAS1-12995
McDonnell Aircraft Company (MCAIR)
McDonnell Douglas Corporation, St. Louis, Mo. 63166
for
NATIONAL AERONAUTICS AND SPACE ADMINISTRATION
Langley Research Center, Hampton, Va. 23865

FOREWORD

This report summarizes the results of "A Fuselage/Tank Structure Study For Actively Cooled Hypersonic Cruise Vehicles" performed from 11 March 1974 through 30 June 1975 under National Aeronautics and Space Administration Contract NAS-1-12995 by McDonnell Aircraft Company (MCAIR), St. Louis, Missouri, a division of McDonnell Douglas Corporation.

The study was sponsored by the Structures and Dynamics Division with Dr. Paul A. Cooper as Study Monitor and Mr. Robert R. McWithey as Alternate Study Monitor.

Mr. Charles J. Pirrello was the MCAIR Study Manager with Mr. Allen H. Baker as Deputy Study Manager. The study was conducted within MCAIR Advanced Engineering which is managed by Mr. Harold D. Altis, Director, Advanced Engineering Division. The study team was an element of Advanced Systems Concepts, supervised by Mr. Dwight H. Bennett.

The basic purpose of this study was to evaluate the effects of fuselage cross section (circular and elliptical) and structural arrangement (integral and non-integral tanks) on the performance of actively cooled hypersonic cruise vehicles. The study was conducted in accordance with the requirements and instructions of NASA RFP 1-08-4129 and McDonnell Technical Proposal Report MDC A2510 with minor revisions mutually agreed upon by NASA and MCAIR. The study was conducted using customary units for the principal measurements and calculations. Results were converted to the International System of Units (S.I.) for the final report.

This is one of three reports detailing the technical results of the study. The other two reports are "Aircraft Design Evaluation," Reference (1), and "Active Cooling System Analysis," Reference (2).

The primary contributor to the contents of this report was Allen H. Baker. Assistance was provided by Robert S. Behrens.

TABLE OF CONTENTS

TABLE OF CONTENTS
(Continued)

TABLE OF CONTENTS
(Continued)

LIST OF ILLUSTRATIONS

LIST OF ILLUSTRATIONS
(Continued)

LIST OF ABBREVIATIONS AND SYMBOLS

ABBREVIATIONS

BFDGW	Basic Flight Design Gross Weight
BL	Buttock Line
CASD	Computer Aided Structural Design
CRT	Cathode Ray Tube
DW	Design Weight
FS	Fuselage Station
MS	Margin of Safety
O.W.E.	Operating Weight, Empty
NM	Nautical Mile
TOGW	Takeoff Gross Weight
WL	Water Line

SYMBOLS

a	Ellipse Major Axis Length
A	Area
b	Ellipse Minor Axis Length
D	Stiffness Parameter - EI
da/dn	Crack Growth Rate
E	Young's Modulus
ft	Foot
°F	Temperature Unit - Degrees Fahrenheit
F_{TU}	Ultimate Tensile Strength
F_{TY}	Yield Tensile Strength
g	Acceleration due to gravity
h	Height
in	Inch
I	Moment of Inertia
K_c, K_{ic}	Critical Stress Intensity Factors
ΔK	Stress Intensity Factor
K_T	Stress Concentration Factor
L	Length
lbf	Pounds Force
lbm	Pounds Mass
M	Bending Moment

LIST OF ABBREVIATIONS AND SYMBOLS (Continued)

ABBREVIATIONS

N	Running Load
n	Load Factor
psi	Pounds force per square inch
P	Axial Load
q	Shear Flow
Q	Shear Load
R	Radius

GREEK SYMBOLS

Δ	Change
ρ	Density

SI UNITS

g	Gram (Weight)
K	Kelvin (Temperature)
m	Meter (Length)
N	Newton (Force)
Pa	Pascal (Pressure and Stress)
W	Watt (Power)

SI PREFIXES

c	Centi (10^{-2})
G	Giga (10^{9})
k	Kilo (10^{3})
m	Milli (10^{-3})
M	Mega (10^{6})

SUBSCRIPTS

c	Compression
cr	Critical
p	Pressure
s	Shear
t	Tension
X	Aircraft Axis - Longitudinal
Y	Aircraft Axis - Lateral
Z	Aircraft Axis - Vertical

1. INTRODUCTION

This report, entitled "Structural Analysis," presents the structural design and analysis studies conducted for each of the three aircraft concepts described in Reference (1). The results of these studies were used in the structural design synthesis of each of the aircraft concepts. In general, while there were some differences, the analytical effort for all three concepts was quite similar.

The effort was directed toward two primary goals:

a. Definition of structural arrangement in the three study aircraft to permit the effects of integral and non-integral hydrogen tankage on vehicle performance to be evaluated.

b. Analytical refinement of structural sizes in the fuselage/tank area in sufficient depth to disclose, with reasonable accuracy, the relative differences in range capability among the three aircraft concepts.

Both goals were first accomplished on the Concept 1 aircraft which had a "Dee" cross section fuselage resulting from the integration of a low wing with circular non-integral fuel tanks. As previously stated, this aircraft was configured to carry a payload of 200 passengers with a mission goal of 9.26 Mm (5000 NM) at a cruise speed of Mach 6.0. The design synthesis and the thermodynamic and structural refinement processes resulted in a range of 8.69 Mm (4690 NM). The Concept 1 design was submitted to NASA and approved as the baseline for comparison during the remainder of the study.

NASA approval of the Concept 1 aircraft was followed by definition and refinement of the Concept 2 (Circular Fuselage-Integral Tank) and Concept 3 (Elliptical Fuselage-Integral Tank). Concepts 2 and 3 had the same payload as Concept 1 (200 passengers), the same fuel quantity, 108.9 Mg (240,000 lbm), and similar aerodynamic characteristics, to allow independent evaluation of the structural arrangement. The final structural arrangement of each aircraft is described in Section 2. Structural drawings of the fuselage/tank area of these aircraft are included in Reference (1).

One of the first tasks to be accomplished was definition of the structural design criteria. References (3), (4) and (5) were utilized as the primary sources for these criteria, which are presented in Section 3. Also included in Section 3 are the structural assumptions and guidelines used in the design of the aircraft concepts.

Another of the initial tasks for this study was selection of structural materials for the aircraft. Descriptions of the initial screening process, the basis for material selection, and the design allowables are provided in Section 4. Section 5 provides the rationale for selection of design loading conditions and defines the loads used for design and analysis of each study aircraft.

One of the most important aspects of the structural analysis on this program was a series of trade studies aimed at getting maximum utilization out of the aircraft volume and structural materials. Section 6 describes these trade studies and assesses the results in terms of weight and aircraft range. Included in Section 6 are trades aimed at selection of the tank configuration and construction, and the actively cooled panel concepts.

The structural analysis to establish detailed structural weights for the fuselage/tank area of each of the aircraft is discussed in Section 7. The intent was to establish structural weight in enough depth that a valid comparison of the range capabilities of the aircraft could be made. The process, which started with creation of a finite element computer model of the fuselage/tank area, is described for each aircraft concept. Transformation of the Section 5 loads into input computer vectors is discussed and illustrated. Weight refinement, based on strength analysis of representative components using computer generated internal load distributions, is also included.

In Section 8 the effects of fatigue, fracture mechanics and creep analysis are discussed.

The conclusions resulting from structural analysis and recommended areas for future investigation are discussed in Section 9.

2. SUMMARY AND STRUCTURAL DESCRIPTION

The purpose of the fuselage/tank structure study was to evaluate the effects of fuselage cross section (circular and elliptical) and structural arrangement (integral and non-integral tanks) on the performance of actively cooled hypersonic cruise vehicles. The fuselage/tank area was analyzed in sufficient detail for a valid assessment of the structural differences between the three study aircraft concepts. Every effort was made to most efficiently use structural components and materials in each concept. Basic differences in design, structural arrangement, and active cooling system concepts are discussed in References (1) and (2). The study results are summarized in Reference (6).

This section describes the structure of the fuselage/tank area in each aircraft concept, points out areas affected by structural trade studies, and briefly describes structural differences. Drawings, including details of each structure, are included in Section 6 of Reference (1).

2.1 CONCEPT 1 FUSELAGE/TANK STRUCTURE

The Concept 1 aircraft fuselage/tank area (center fuselage) structure consists of a full monocoque shell surrounding two non-integral, circular cross section, liquid hydrogen (LH_2) tanks. An exploded view of the structure is presented in Figure 1.

The shell is composed of aluminum honeycomb sandwich actively cooled panels, which are supported at approximately 0.91 m (3 ft) intervals by 0.15 m (6 in.) deep aluminum frames. The frames are attached directly to the upper surface of the wing carry-through, which forms the majority of the lower portion of the center fuselage shell. The fuselage frames and the actively cooled panel covering continue around the tanks in areas away from the wing carry-through. The continuous wing carry-through was selected for Concept 1, instead of using fuselage frames for that purpose, because previous studies of aircraft such as the F-4 and F-15 had showed significant weight savings for this structural arrangement.

The center fuselage shell is the primary redistribution member for wing, landing gear, engine nacelle, and non-integral fuel tank loads. The vertical tail and the forward and aft fuselage sections are spliced to it to complete the structural assembly. The shell was designed as a safe-life structure, that is, one in which a defect will not grow to structural failure in the

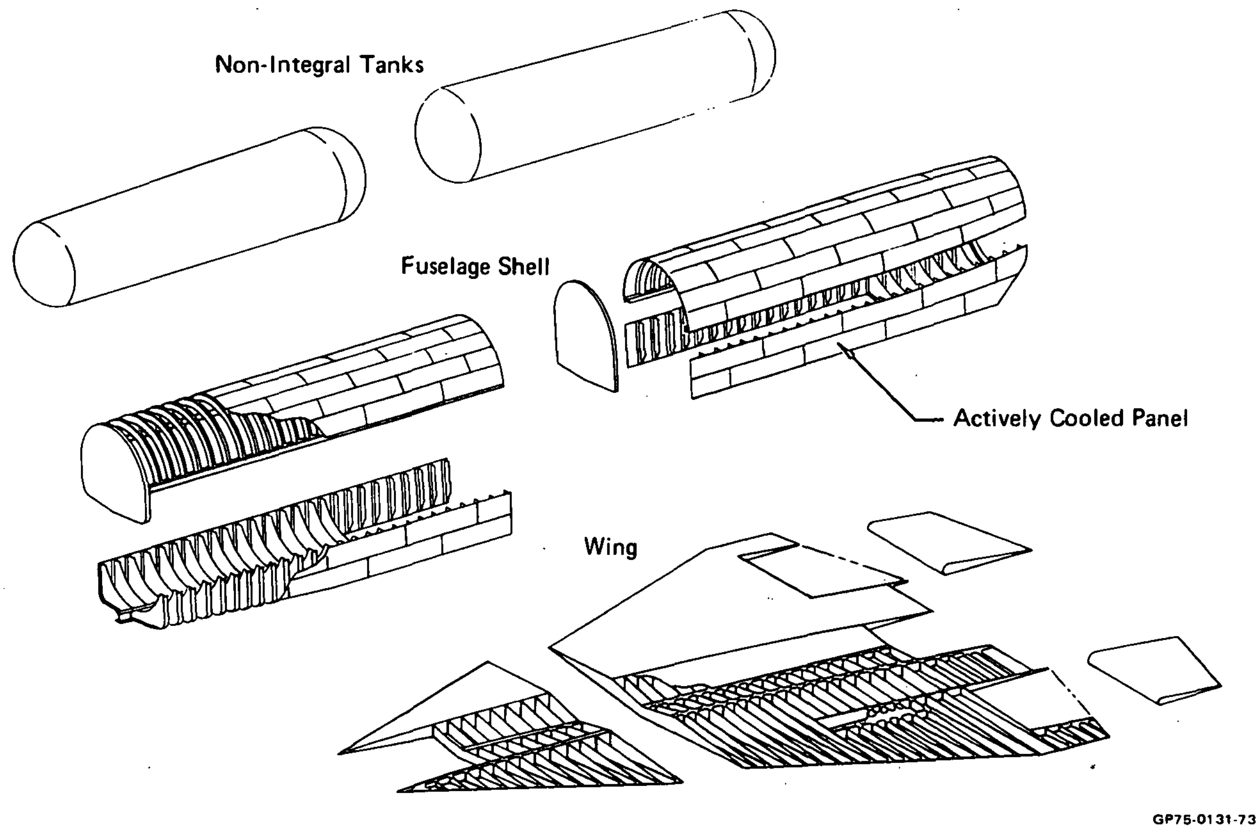

Note: Detailed drawings of this structure may be found in section 6 of Reference (1)

FIGURE 1
FUSELAGE/TANK AREA STRUCTURE - CONCEPT 1

2500 flight hour interval between structural inspections. The impact of this design requirement is discussed in Section 8.3.

Figure 2 shows, in some detail, the construction of the actively cooled panels used as moldline covering on the study aircraft. It was selected as a result of a structural trade study described in Section 6.2.4. Each panel is an adhesively bonded assembly with "Dee" shaped tubes along the moldline surface which carry coolant to keep the surface at a maximum temperature of 394 K (250°F). The panel ends are formed by structural coolant manifolds which either distribute or collect the panel coolant flow. The entire actively cooled panel assembly is constructed from aluminum alloys.

The two non-integral liquid hydrogen tanks have monocoque shells and the tank ends are elliptically domed. The structural trade studies leading to this configuration are discussed in Section 6.2.2. Each tank is mounted to the fuselage structure at four points, with reactions controlled in such a manner that tank support is statically determinate. Longitudinal members at each side of the tank redistribute concentrated tank reaction loads. This support method, illustrated in Figure 3, prevents tank loads from being induced by fuselage bending or thermal differentials. This dimensional freedom also permits liberal manufacturing tolerances. The Concept 1 fuel tanks were designed to burst pressure requirements and were not limited by fatigue or fracture mechanics criteria.

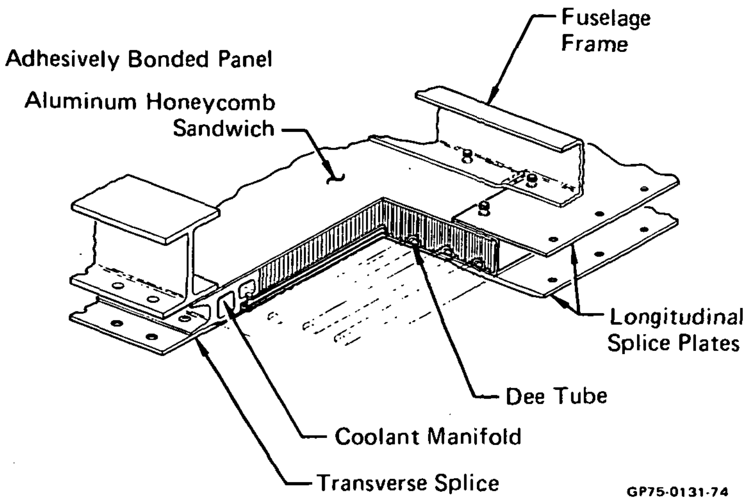

FIGURE 2
ACTIVELY COOLED PANEL CONSTRUCTION

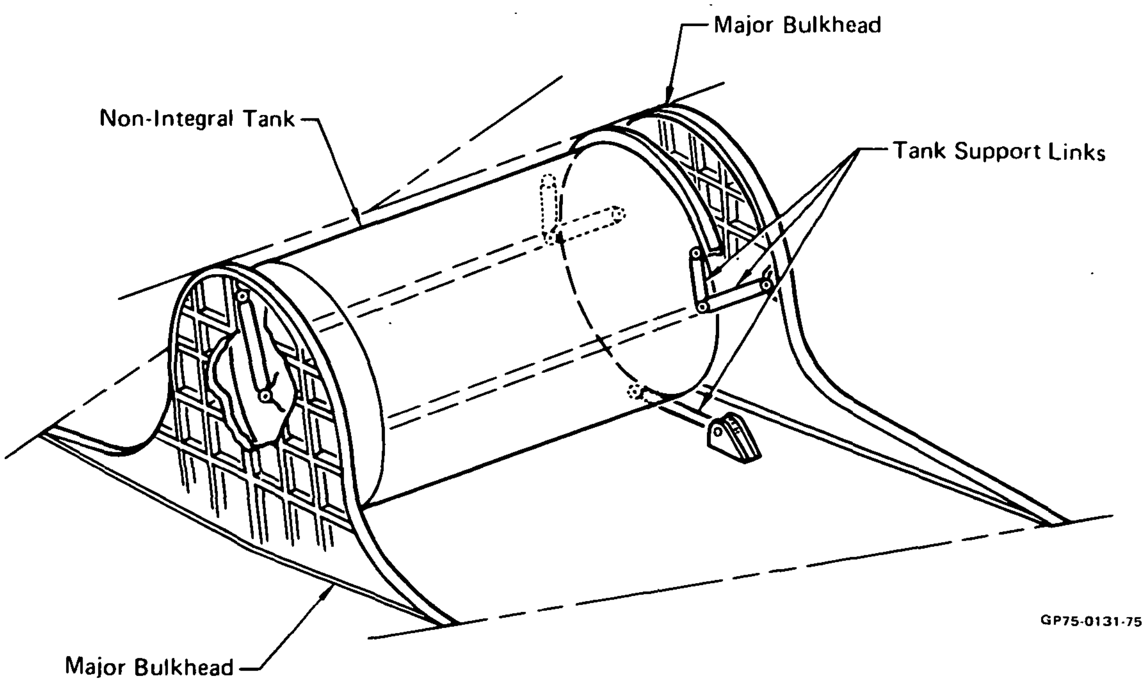

FIGURE 3
NON-INTEGRAL TANK SUPPORT

2.2 CONCEPT 2 FUSELAGE/TANK STRUCTURE

The Concept 2 aircraft is almost identical in external appearance to Concept 1. The structural arrangement of the fuselage/tank area is quite different, however, as shown in Figure 4. A single integral fuel tank serves as the main load carrying member for the center fuselage. It redistributes loads from all the appurtenant aircraft members but, unlike Concept 1, these members are not all at the same structural temperature. The tank is encapsulated by external insulation and is maintained at the 20.3 K (-423°F) temperature of the liquid hydrogen fuel. The remaining structure is composed of actively cooled panels at an average temperature of 366 K (200°F) in cruise flight.

Such a temperature differential in aluminum structure produces thermal strains totaling nearly 0.006 $\frac{cm}{cm}(\frac{in}{in})$. In conventional structure those strains would equate to thermal stresses well in excess of yield strength. In Concept 2, however, the structure has been interconnected with link systems that accommodate the thermal strains while still maintaining reliable structural load paths.

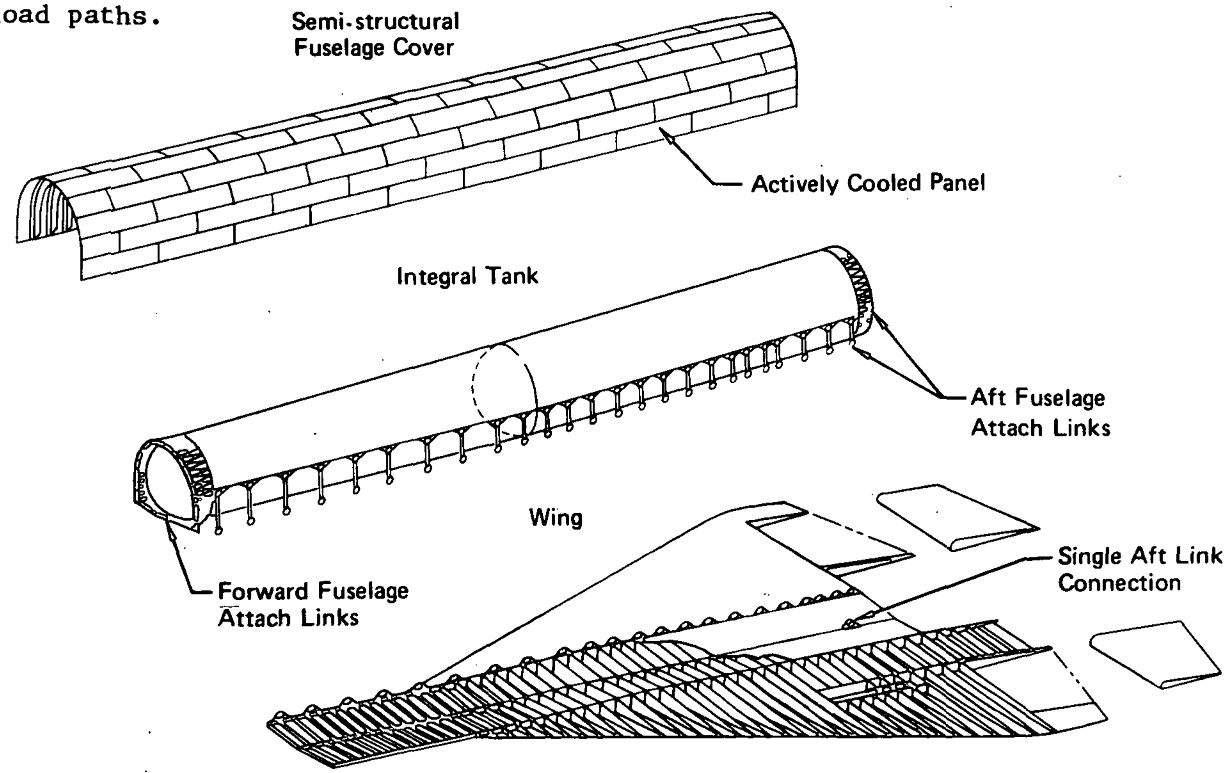

Note: Detailed drawings of this structure may be found in section 6 of Reference (1)

GP75-0131-76

FIGURE 4
FUSELAGE/TANK AREA STRUCTURE - CONCEPT 2

As an example the wing-to-tank connection is made with a series of links which have monoball bearings at each end to allow the links to swivel and yet allow one end of the link to move with respect to the other. Each link has full axial load capability. As indicated in Figure 4, a series of nearly vertical links is used to attach each side of the fuel tank to the upper surface of the wing. The longitudinal location of the tank is fixed by a single aft link which attaches to the wing carry-through at the centerline. Side motion of the tank is prevented by a series of transverse links. Details of the link arrangement can be found in Section 6 of Reference (1).

Thermal contraction of the tank is accommodated by these links, which travel in an arc and induce a bending stress of only about 3.45 MPa (500 psi) in the tank at the peak of the arc. A truss network formed of the same type of links provides thermal strain relief at the splice joints where the forward and aft fuselage sections and the vertical tail attach to the tank.

The tank itself is divided into two sections. The divider and the tank ends are elliptically domed, as they were on the Concept 1 aircraft. The internal divider is used to provide aircraft center of gravity control and also to reduce the crash landing pressure head loads. Tank walls are integrally stiffened, using an Isogrid pattern as illustrated in Figure 5. This method of stiffening was found to be the lightest as the result of a structural trade study, discussed in Section 6. Concept 2 tanks were critical for fatigue analysis as shown in Section 7.

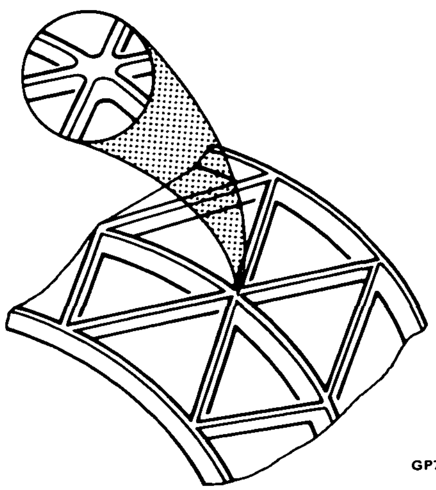

FIGURE 5
ISOGRID TANK WALL STIFFENING

The upper tank covering consists of actively cooled panels which are assembled and attached to the wing in the same manner as on the Concept 1 aircraft. A trade study, reported in Section 6.3.2, determined that considerable tank weight could be saved by using these panels as secondary bending structure. The panels have a thickness of 1.27 cm (0.5 in.) rather than the 2.03 to 4.06 cm (0.8 to 1.6 in.) that was required on the Concept 1 aircraft.

One design consideration was that, with the method of aircraft primary structure assembly shown in Figure 4, the forward and aft fuselage sections would move toward each other when the tank was filled with cryogenic fuel. This requires that the upper tank covering have a variable length. A compromise was reached which made the cover "semi-structural" to accommodate length change. The panels were attached to each other and to the wing in the same manner as on Concept 1, but the cover was ended before it reached the forward and aft fuselage splice joints. Slip joints were then added to allow relative motion. No shear, bending moment, or axial load is introduced at either end; hence the "semi-structural" classification. Details of this construction are shown in Reference (1). The loads induced into the tank cover are quite low and the thinner cover structure is not critical for stability.

2.3 CONCEPT 3 FUSELAGE/TANK STRUCTURE

The liquid hydrogen fuel tank is the primary structure in the center fuselage in Concept 3, as it was in Concept 2. It also acts as the wing carry-through. Wing and forward and aft fuselage attachments are made with link systems similar to those used on Concept 2, to relieve thermal strains.

The LH_2 tank has a five bubble cross section. The trade study leading to the selection of this configuration is discussed in Section 6.4.2. Tank walls are stiffened in an Isogrid pattern, and the divider and end domes are elliptical, as they were on Concept 2. Material was added to several of the rings which act as the wing carry-through as a result of fatigue allowable stresses. The effect of this addition is noted in Section 8. Internal webs at the circular intersections are constructed of stiffened sheet metal and are mechanically attached.

A "semi-structural" configuration was considered for the tank covers on Concept 3, but preliminary layouts showed the support structure would either be marginal in weight saving or be too complex to be practical. It was decided then to support each panel individually from the multi-bubble tank, in essentially the same manner as tank-to-wing connection for Concept 2. Slip joints were added around the perimeter of each panel, but are required to accommodate only limited motion compared to those on the Concept 2 configuration.

Details of the Concept 3 structural arrangement can be found in Section 7 of Reference (1).

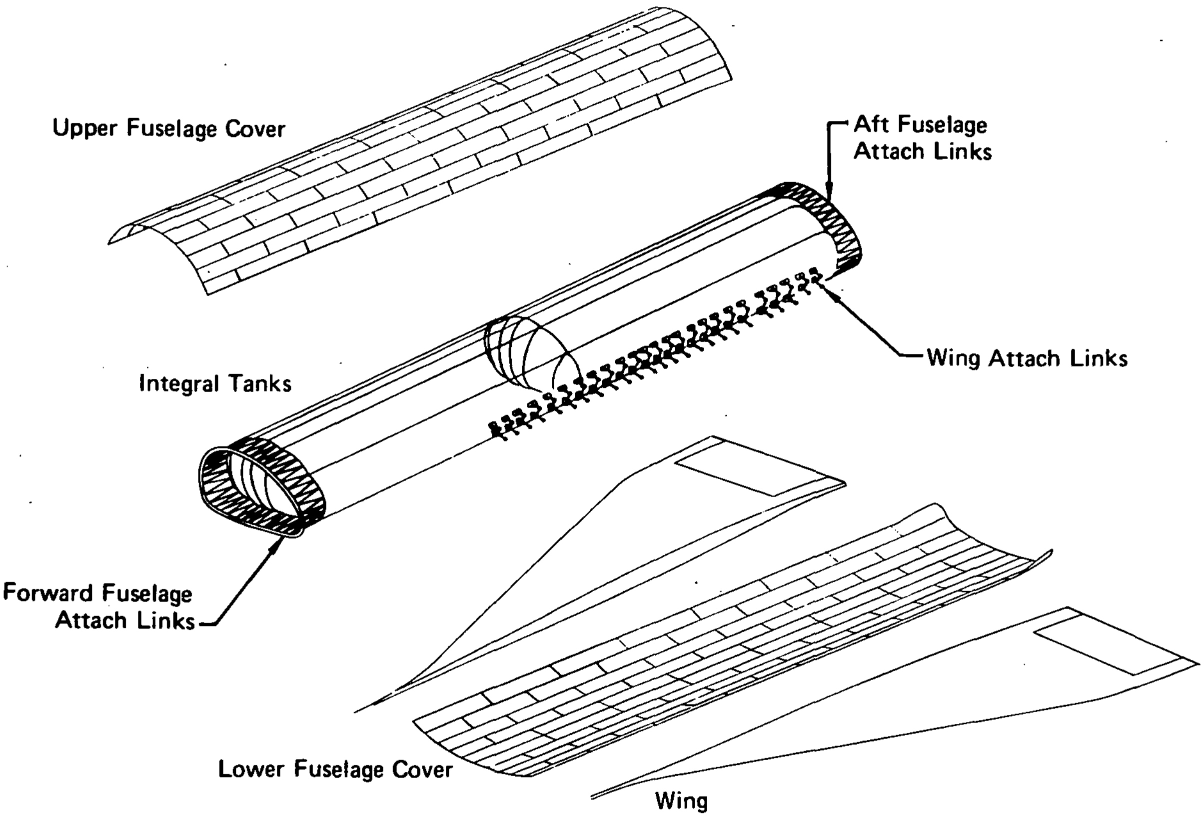

Note: Detailed drawing of this structure may be found in section 6 of Reference (1)

GP75-0131-78

FIGURE 6
FUSELAGE/TANK AREA STRUCTURE - CONCEPT 3

3. STRUCTURAL DESIGN CRITERIA

The structural design criteria for this program follows Paragraph 4.2 of Reference (3): "Design criteria for the vehicle concepts shall be consistent with, as far as practical, those outlined in Federal Aviation Regulations, Volume III, Part 25, Airworthiness Standards: Transport Category Airplanes Reference (4), and NASA document SP-8057 NASA Space Vehicle Design Criteria (Structures) Reference (5)."

3.1 GENERAL CRITERIA

3.1.1 Design Load Factors - Design load factors for the aircraft were as follows:

a. Flight n_z = 2.5, -1.0 (Limit)

b. Taxi Bump n_z = 2.0 (Limit)

c. Emergency Landing (Ultimate) n_z = 4.5, -2.0, n_x = 9.0, n_y = $\pm$ 1.5

Load factors are defined as positive if the acceleration is upward (n_z) or forward (n_x).

3.1.2 Weight Definition - Takeoff Gross Weight (TOGW) is defined, Reference (7), as the weight of the airplane with maximum internal load with no reduction permitted for fuel used during taxi, warm-up, or climb-out. This weight is also assumed to be equal to Basic Flight Design Gross Weight (BFDGW). Although this is conservative, it does provide for a valid comparison between the study aircraft. The fact that current transport aircraft are allowed to taxi at greater than TOGW was not felt to be significant to the comparisons made for this study. For simplicity this weight is called design weight (DW) in this report.

3.2 FUEL TANK PRESSURIZATION

The fuel tanks were pressurized to a limit pressure of 138 kPa (20 psi) gage per Reference (3).

3.3 PURGE REQUIREMENTS

Configurations with a void between the outer surface and the tankage structure (non-integral tank configuration), were designed for a maximum limit purge-gas gage-pressure of 3.45 kPa (0.5 psi) in the void space, Reference (3).

3.4 FACTORS OF SAFETY

Factors of safety used for design and analysis are:

3.4.1 General Structure Combined With Tank Loads - (Applies to integral or non-integral tanks).

Limit structure loads (Factor of Safety = 1.0) combined with limit tank pressures (Factor of Safety = 1.0) do not result in principal stresses greater than yield.

Ultimate structure loads (Factor of Safety = 1.5) combined with limit tank pressure (Factor of Safety = 1.0) were used in computing ultimate margins of safety.

3.4.2 Fuel Tank Pressure - The factor of safety used for burst pressure analysis was 2.0.

3.4.3 Thermally Induced Loads - Limit Factor of Safety = 1.0, Ultimate Factor of Safety = 1.0.

3.5 FATIGUE AND FRACTURE MECHANICS REQUIREMENTS

3.5.1 Service Life - Aircraft service life used for fatigue was 10,000 flight hours, Reference (3). Aircraft service life used for fracture mechanics (crack growth) was 2500 flight hours, on the premise that there will be a complete structural inspection of each vehicle after each 2500 flight hours. A scatter factor of 4.0 was applied, Reference (5), Paragraph 4.7.1. Therefore the design lives for fatigue and fracture mechanics analyses were 40,000 and 10,000 flight hours, respectively.

3.5.2 Fatigue Spectrum - The fatigue spectrum selected for this study is shown in Figure 7. The spectrum was based upon the one used for analysis and testing of the DC-10, but with the 120,000 hour life reduced to the 40,000 hours required for the study aircraft. Ground-air-ground cycles were added as appropriate to the hypersonic aircraft.

Analyses were limited to the immediate fuselage/tank area, and only vertical load factors resulting from maneuvering, gusts, and ground-air-ground cycles were included in the fatigue spectrum. Side loads were not considered in this study.

DC-10 maneuvering spectra were derived from usage of commercial jet transports and should be directly applicable to this study. DC-10 gust loading spectra are based on a power spectral density (PSD) analysis of the atmospheric turbulence which would be encountered during its service life. The study aircraft was shown to be less responsive to vertical gusts than the DC-10. Hence, use of the DC-10 spectrum was conservative for this study.

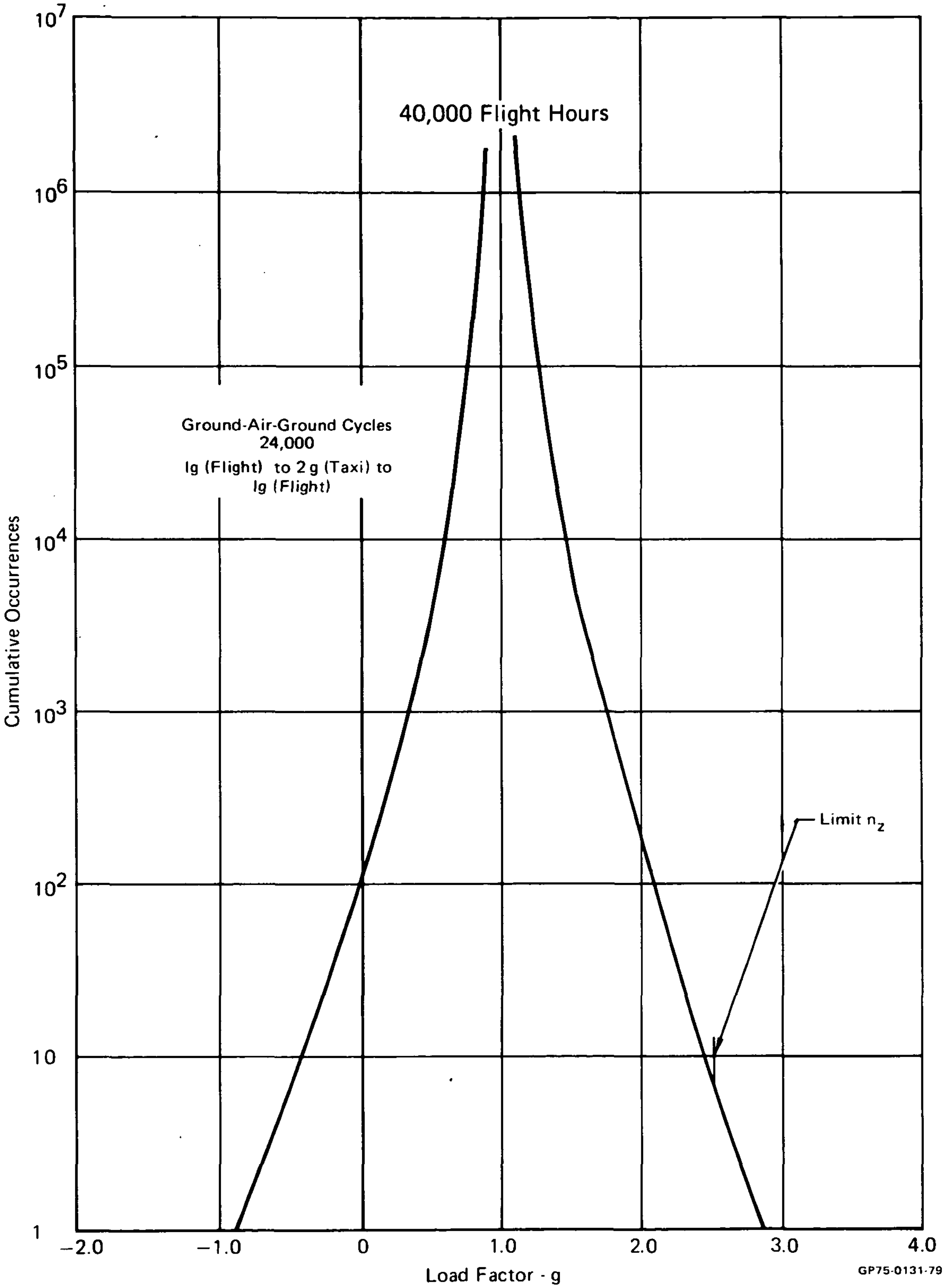

FIGURE 7
VERTICAL LOAD FACTOR SPECTRUM

Ground-air-ground cycles were arbitrarily defined as going from a one g flight condition to 2 g's on the ground in a three point taxi condition and back to one g in flight. The minimum flight time for the study aircraft is expected to be approximately 6000 seconds (1.67 hrs) so 6000 flights were assumed per 10,000 hour lifetime. 24,000 ground air-ground cycles were therefore included in the design fatigue spectrum, which includes a scatter factor of four on aircraft service life.

3.6 DESIGN TEMPERATURES

Structural temperatures used for design were the calculated values with maximum cooled surface temperature limited to 394K (250°F), Reference (3).

3.7 LOADING CONDITIONS

Loading conditions used for design and analysis were defined as follows:

a. A symmetrical pullup, performed at DW, which produces maximum fuselage bending moments. Selection of the design point on the ascent trajectory was based on aerodynamic analyses of the Concept 1 aircraft. That design point was then held constant for the remainder of the study and was felt to provide adequate information for valid comparison of the three study aircraft. Cruise maneuvers, other than minor course corrections, were considered to be abnormal and beyond the scope of this study.

b. A taxi or landing condition at DW which produces maximum fuselage bending moments in the area of the main landing gear.

c. An emergency landing (crash) condition which produces maximum loading on items that must be retained in the aircraft, such as non-integral fuel tanks.

d. Unsymmetrical loading conditions were not considered significant to assure valid study comparisons. Thus they were not considered.

3.8 PERTINENT ASSUMPTIONS AND GUIDELINES

3.8.1 Fuel - It was assumed that the fuel for the study aircraft concepts is normal boiling point hydrogen at a temperature of 20.3 K (-423°F). It has further been assumed for purposes of structural analysis that the hydrogen tanks are always pressurized.

3.8.2 Passenger Cabin Pressurization - It was assumed that passenger cabin pressurization requirements of Reference (4) would be essentially the same for the three aircraft concepts.

3.8.3 Fail-Safe vs Safe-Life Analysis - Fail-safe vs safe-life analysis, when conducted, used the definitions and failure mechanisms of Reference (5). Fail-safe structure was defined as the capability of sustaining 100% limit load after a single failure and still having a safe-life of 2500 flight hours. Safe life structure was defined as having an analytical life, either in fatigue or fracture mechanics analysis, equal to or greater than the aircraft design life.

3.8.4 Creep Analysis - Creep analysis was required to show 0.5% or less creep in the design service life of the study aircraft.

3.8.5 Baffling - Baffling for all three tank configurations as assumed to be similar, and was excluded from analytical consideration.

3.8.6 Thermal Stress - Thermal stress in the tanks was considered negligible, since it was estimated that a 56 K (100°F), or less, temperature differential exists at the liquid/gaseous hydrogen interface. Tank wall temperature gradients of this magnitude do not generate significant thermal stresses.

4. MATERIAL SELECTION

One of the first tasks was the selection of materials to be used for primary and secondary structure. Reference (4) limited the primary structure to aluminum alloys, so investigation was centered in that area. Annealed titanium alloy 6Al-4V was considered, however, for limited application, such as fuselage links and fittings, where concentrated loads occur and lighter structure would result. The 6Al-4V alloy was selected because of its favorable combination of tensile strength, high fatigue allowables, and good fracture toughness, compared to several commonly used titanium alloys.

Material selection was based primarily on Concept 1 requirements. The selection was kept constant for all concepts so that material properties would not be a variable in the final comparison and evaluation. That assumption was reviewed as the design of Concepts 2 and 3 progressed. No special design requirements were found which would make the original selection invalid.

Two major considerations were paramount in selection of the aluminum alloys to be used on the Concept 1 aircraft. Those were the 394K (250°F) maximum temperature to which the moldline structure was to be cooled and the cryogenic 20.3K (-423°F) temperature at which the fuel tanks would operate. A third consideration was the decision to assemble the tanks by welding. This provided the best vapor seal against leakage of the hydrogen fuel and minimized the weight of the joints required in assembling the large tanks. Section 4.1 discusses the elevated temperature considerations and Section 4.2 the cryogenic application of weldable alloys. Section 4.3 presents material properties of the selected materials used for design.

4.1 SELECTION OF ALUMINUM ALLOY FOR ACTIVELY COOLED PANEL CONSTRUCTION

A comparison was made of material properties for several aluminum alloys showing promise for primary structure. A summary of that comparison can be found in Figure 8. Based on this comparison, 2014-T6 and 7075-T6 alloys were eliminated because of their susceptibility to corrosion and stress corrosion cracking. The 7475-T761 material was not competitive with the 2000 series alloys from an elevated temperature strength standpoint and had the additional disadvantage of being available from only a single source with resulting high cost. Low strength properties at both room and elevated temperatures eliminated the 6061-T6 material and the T6 temper of the 2219 alloy.

Material	Fatigue (20,000 Cycles)	K_C	da/dn ($\Delta K = 30$)	F_{TU}/ρ	F_{TY}/ρ	F_{CY}/ρ	$E_C^{0.333}/\rho$	$(E_C^{0.325} F_{CY}^{0.325})/\rho$	Advantages	Disadvantages
	T = 300K (80°F)			T = 394K (250°F) (10,000 Hrs)						
2014-T6	1.00	0.67		0.92	0.84	0.99	0.99	1.00		Susceptible to corrosion, exfoliation, and stress corrosion cracking
2024-T81	1.00	0.47	0.34	1.00	1.00	1.00	1.00	1.00	Good corrosion resistance, good elevated temperature mechanical properties	Low fracture toughness at room temperature. No elevated temperature fracture toughness data
2219-T6	0.64	0.92		0.75	0.58	0.63	0.98	0.86	Stable for long time exposure at elevated temperature	Low initial strength, i.e., at low temperatures. No Elevated temperature K_C data
2219-T87	1.00	0.98	1.00	0.79	0.77	0.82	0.98	0.95	High fracture toughness, stable for long time exposure to elevated temperature. good corrosion resistance weldable, property data readily available at elevated temperature	Low initial strength, i.e., at low temperatures. No elevated temperature K_C data
6061-T6	0.69	1.00	0.41	0.59	0.57	0.61	1.00	0.85	High fracture toughness. Excellent corrosion resistance	Low strength. No elevated temperature K_C data
7075-T6	0.91	0.60	0.76	0.84	0.82	0.80	0.98	0.95		Susceptible to corrosion. Exfoliation, and stress corrosion cracking. Low fracture toughness. Temperature limited. No elevated temperature K_C data.
7475-T761	0.78	0.89	1.00	0.59	0.76	0.85	0.97	0.88	High fracture toughness	Sole source, premium price, temperature limited. No elevated temperature K_C data

Note: Index rating ratio property to highest value in column. Highest number is best rating

GP75-0131-80

FIGURE 8
SUMMARY MATERIAL EVALUATION - ELEVATED TEMPERATURE

This left only the 2024-T81 and 2219-T87 materials for serious consideration as the basic construction material for the actively cooled panels. The failure modes expected to be most significant were stability, with (E_c) compressive modulus of elasticity being the figure of merit, and fracture mechanics, with crack growth rate (da/dn) and fracture toughness coefficient (K_c) being the figures of merit. The 2219-T87 alloy was shown to be competitive in stability parameters and to have a definite superiority over 2024-T81 in fracture mechanics. 2219-T87 was therefore selected as the construction material for those structural elements operating at elevated temperature.

4.2 SELECTION OF ALUMINUM ALLOY FOR CRYOGENIC TANK CONSTRUCTION

The choice of materials for cryogenic tank construction was limited by the aforementioned decision to utilize all-welded construction. A comparison of the three candidate materials is presented in Figure 9. From this comparison it became obvious that the crack growth characteristics (da/dn) of 6061-T6 would quickly eliminate it from further consideration. The 2014-T6 material was also eliminated because of its inherent susceptibility to corrosion and stress corrosion cracking. 2219-T87 aluminum alloy was chosen as the most acceptable material for tank fabrication.

	T = 300K (250°F)			T = 20.3K (−423°F)					
Material	Fatigue (20,000 Cycles)	K_C	da/dn ($\Delta K = 30$)	F_{TU}/ρ	E_C/ρ	K_{IC}/ρ	Fatigue (20,000 Cycles)	Advantages	Disadvantages
2014-T6	1.0	0.67		1.0	0.98	0.80	1.0		Susceptible to corrosion, exfoliation, and stress corrosion cracking
2219-T87	0.64	0.98	1.0	0.99	1.0	1.0	0.94	High fracture toughness, stable for long time exposure to elevated temperature. Good corrosion resistance weldable, property data readily available at elevated temperature	Low room temperature strength
6061-T6	0.69	1.0	0.41	0.67	0.99		0.83	High fracture toughness. Excellent corrosion resistance	Low strength. No cryogenic temperature K_C data

Note: Index rating-ratio of property to highest value in column. Highest number is best rating

GP75-0131-81

FIGURE 9
SUMMARY MATERIAL EVALUATION - CRYOGENIC TEMPERATURE

4.3 MATERIAL ALLOWABLES USED FOR DESIGN

Figure 10 presents a tabulation of the 2219-T87 material allowables used for design of the study aircraft. In each of the tension loading cases the allowable stress was the least of three values: (a) Ultimate Tensile Stress, (b) 1.5 times the Fatigue Design Allowable stress at the stress concentration factor noted, or (c) 1.5 times the Fracture Mechanics Design Allowable, based upon the largest flaw with more than a 2% probability of being undetected in detail fabrication. Where fracture mechanics (crack growth) analysis is the basis for an allowable the flaw size is noted. The cryogenic tension allowable for as-welded 2219-T87 was used, in all cases, to provide an analytical method to beef-up weld lands so that the welds were equally critical with the parent material. Adequate weight allowances were made on all three aircraft to account for this beef-up.

Compression allowables for this study are bounded by, but never reach, ultimate tensile strength of the material. Local design of a honeycomb panel or stiffened tank wall was used to analytically determine compression allowables.

Figure 11 provides the allowables used for design of those components for which it was felt that use of 6Al-4V annealed titanium would benefit the study aircraft by reducing weight.

Loading Direction	Temp K (^{o}F)	Material	Allowable Stress MPa (10^3 psi)	Modulus of Elasticity GPa (10^6 psi)	Basis
Tension	366 (200)	Parent	404 (58.6)	68.9 (10)	Ultimate Tensile Strength (F_{tu})
			532(1) (77.2)	68.9 (10)	Fatigue Analysis K_T = 3.06
			176(1) (25.5)	68.9 (10)	Crack Growth Analysis 0.127 mm (0.005 in.) Crack from Fastener Hole
Compression			404 (58.6)	68.9 (10)	Limited by F_{tu} Determined by Local Design
Tension	20.3 (−423)	Parent	652 (94.5)	82.7 (12)	Ultimate Tensile Strength (F_{tu})
			558(1) (81)	82.7 (12)	Fatigue Analysis K_T = 1.50
			393(1) (57)	82.7 (12)	Fatigue Analysis K_T = 3.06
			Not Critical		Crack Growth Analysis 0.25 mm x 6.35 mm (0.01 in. x 0.25 in.) Scratch
		As Welded	290 (42)	82.7 (12)	Ultimate Tensile Strength (F_{tu})
			165(1) (24)	82.7 (12)	Fatigue Analysis K_T = 1.5
			445(1) (66)	82.7 (12)	Crack Growth Analysis 1.27 mm x 0.635 mm (0.05 in. x 0.025 in.) Crack
Compression		Parent	652 (94.5)	82.7 (12)	Limited by F_{tu} Determined by Local Design
Tension	294 (70)	Parent	434.4 (63)	74.46 (10.8)	Ultimate Tensile Strength (F_{tu})
		As Welded	193.1 (28)	74.46 (10.8)	Ultimate Tensile Strength (F_{tu})

(1) Includes 1.5 Factor of Safety for Comparison to Ultimate Loads

GP75-0131-158

FIGURE 10
2219-T87 ALLOWABLE STRESSES

Loading Direction	(1) Allowable Stress MPa (ksi)	Basis
Tension	896 (130)	Ultimate Tensile Strength (F_{tu})
	Not Critical	Fatigue Analysis $K_T = 3.06$
	848 (2) (123)	Crack Growth Analysis 1.27 mm x 0.635 mm (0.05 in. x 0.25 in.) Crack
Compression	896 (130)	Limited by F_{tu} Determined by Local Design

(1) At Room Temperature
(2) Includes 1.5 Factor of Safety for Comparison to Ultimate Loads

Modulus of Elasticity = 110.3 GPa (16 x 10^6 psi)

GP75-0131-159

FIGURE 11
ANNEALED 6Al-4V TITANIUM ALLOWABLE STRESSES

5. AIRCRAFT LOADS

Aircraft loads data were generated to implement structural analysis of the fuselage/tank area of the three study aircraft concepts. Three symmetrical conditions, as indicated in Section 3.7, were selected: (a) a maximum load factor pullup to induce the largest flight bending moments, (b) a ground condition (landing or taxi) to generate maximum bending moments in the area of the main landing gear, and (c) emergency (crash) condition to account for bending analysis and retention of the non-integral tanks.

In this section the rationale for establishment of the Concept 1, 2 and 3 loads is discussed and the results presented.

5.1 CONCEPT 1 LOADS

The flight condition selected for design of Concept 1 was a 2.5g symmetrical pullup at Mach 3 and an altitude of 15.2 km (50,000 ft). This condition is coincident with the maximum dynamic pressure during the ascent trajectory. Ultimate aircraft shear and bending moments for the flight condition are presented in Figure 12. The aircraft was assumed to be at DW.

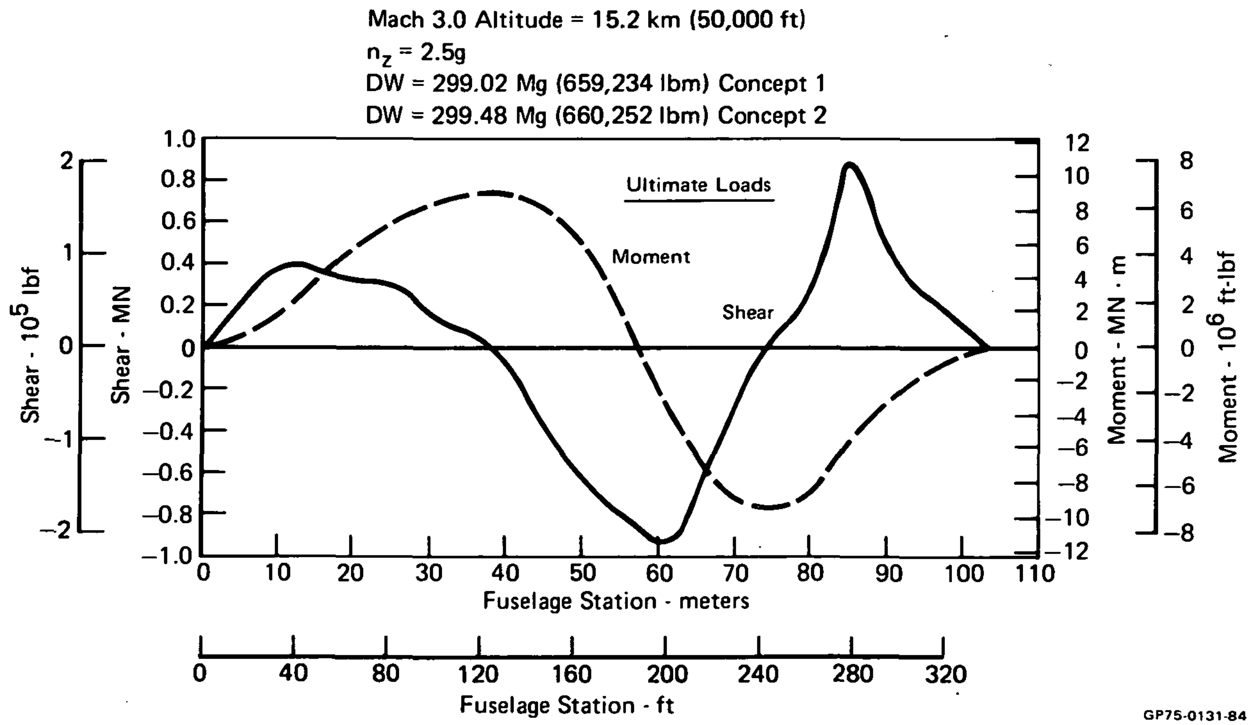

FIGURE 12
CONCEPT 1 AND 2
Net Aircraft Shear and Moment
2.5g Flight Condition

The ground condition resulting in maximum fuselage bending moments was assumed to be a 2.0g bump encountered during taxi. It was assumed that there was no wing lift to relieve the inertia induced bending moments and that the aircraft was at DW.

Ultimate shear and bending moment curves for this condition can be found in Figure 13. Comparison of Figures 12 and 13 shows that the taxi condition creates critical loads in the areas of both the main and nose landing gear. Landing gear location was therefore affected by bending moment considerations. A more normal main landing gear location, which would have allowed the aircraft to rotate for takeoff, would have been considerably farther forward. But such a location would have more than tripled the bending moment in the fuselage/tank area, resulting in an excessive weight penalty. Takeoff and landing performance with the landing gear in the selected position is discussed in Reference (1).

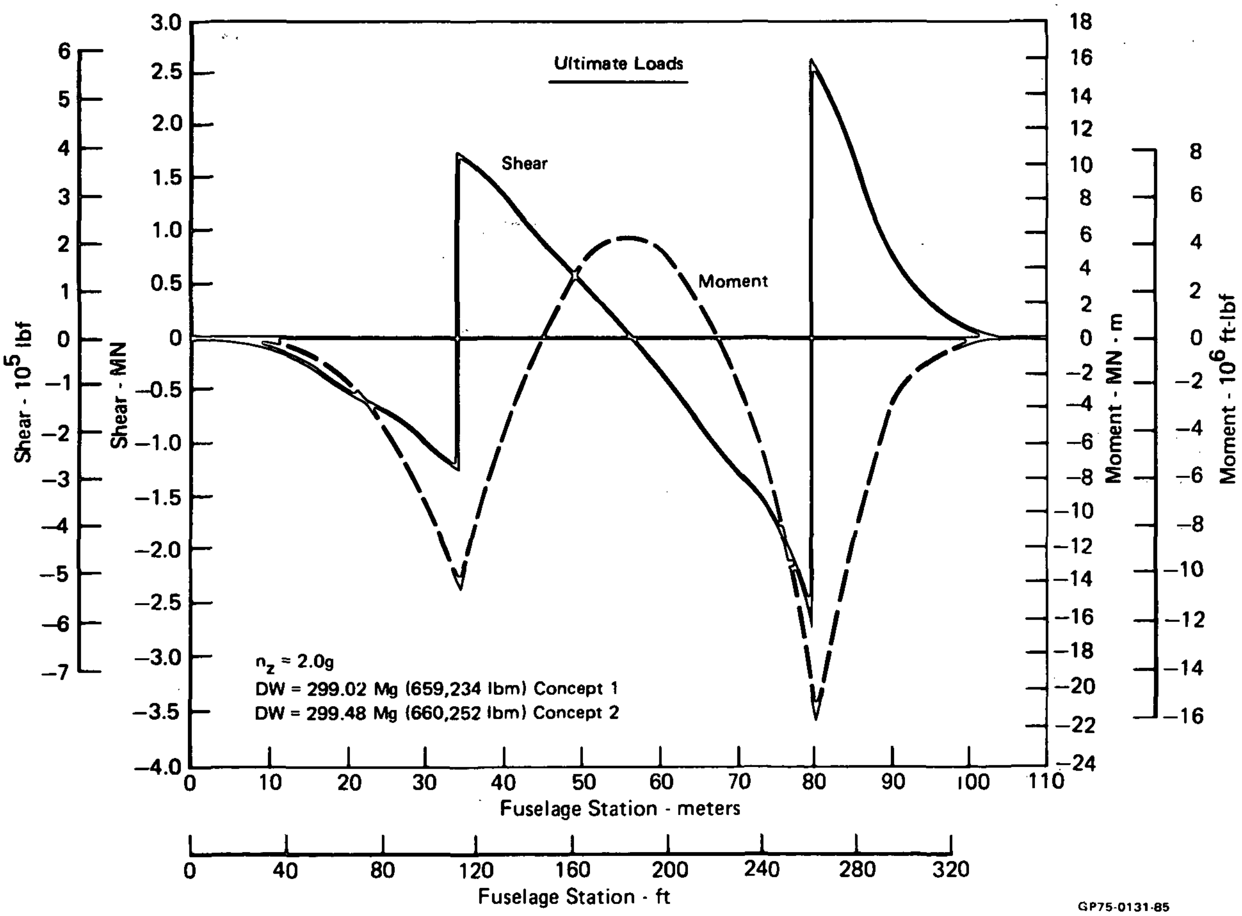

FIGURE 13
CONCEPT 1 AND 2
Net Aircraft Shear and Moment
2g Taxi Condition

The non-integral fuel tanks and support structure of Concept 1 were designed by burst pressure and the crash condition which combines 4.5g acceleration down with 9.0g forward on the tanks themselves. Because of the simple support of the tanks the bending moment can be readily calculated. The peak fuel tank bending moment was 8.724 MN·m (6.435 x 10^6 ft-lbf) and the crash pressure head at the forward end of the tank was 168 kPa (24.4 psi).

Fuel tank strength analysis, based on Section 3 criteria, was performed on the Concept 1 structure, considering that the tanks were always full, at cryogenic temperature, and pressurized to 138 kPa (20 psi) gage.

The space between moldline structure and tanks on the Concept 1 aircraft was considered to be pressurized to 3.45 kPa (0.5 psi).

5.2 CONCEPT 2 LOADS

The flight and ground loading conditions selected for the Concept 2 aircraft were the same as those used for Concept 1. Because the difference in TOGW between the first two aircraft concepts was only 462 kg (1018 lbm), or 0.15% of the total aircraft weight of 299 Mg (660,252 lbm) and because of the identical aircraft lengths it was decided to use the Concept 1 loads for the Concept 2 aircraft. Figures 12 and 13, then, were used for both concepts.

The crash condition was used only to calculate pressure heads in the tank for the Concept 2 aircraft since the tanks were an integral part of the aircraft structure and retention was not a consideration.

Tank and purge pressures used for design of the Concept 2 aircraft were the same as those used for Concept 1.

5.3 CONCEPT 3 LOADS

Again the flight and ground conditions used for design were the same as those selected for Concept 1. However, the Concept 3 aircraft was 3.07 Mg (6775 lbm) lighter than Concept 1 and nearly 13.6 m (30 ft) shorter, so new shear and bending moment loads were generated. Ultimate shear and bending moment curves for Concept 3, for the 2.5g flight and 2.0g taxi bump conditions, are presented in Figures 14 and 15 respectively.

As in Concept 2, tank retention was not a consideration and the crash condition was used only to assure that crash pressure heads were at acceptable levels.

Tank and purge pressures used for design of the Concept 3 aircraft were the same as those used for Concept 1.

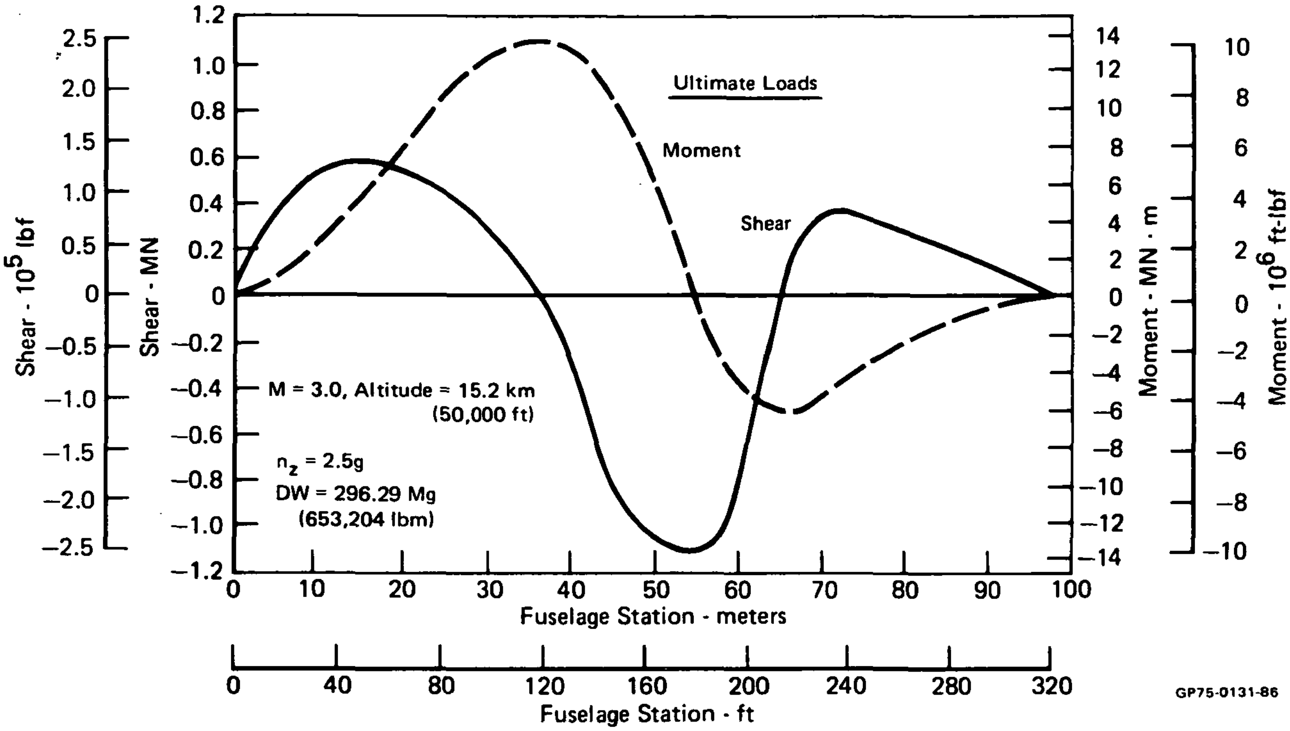

FIGURE 14
CONCEPT 3
Net Aircraft Shear and Moment
2.5g Flight Condition

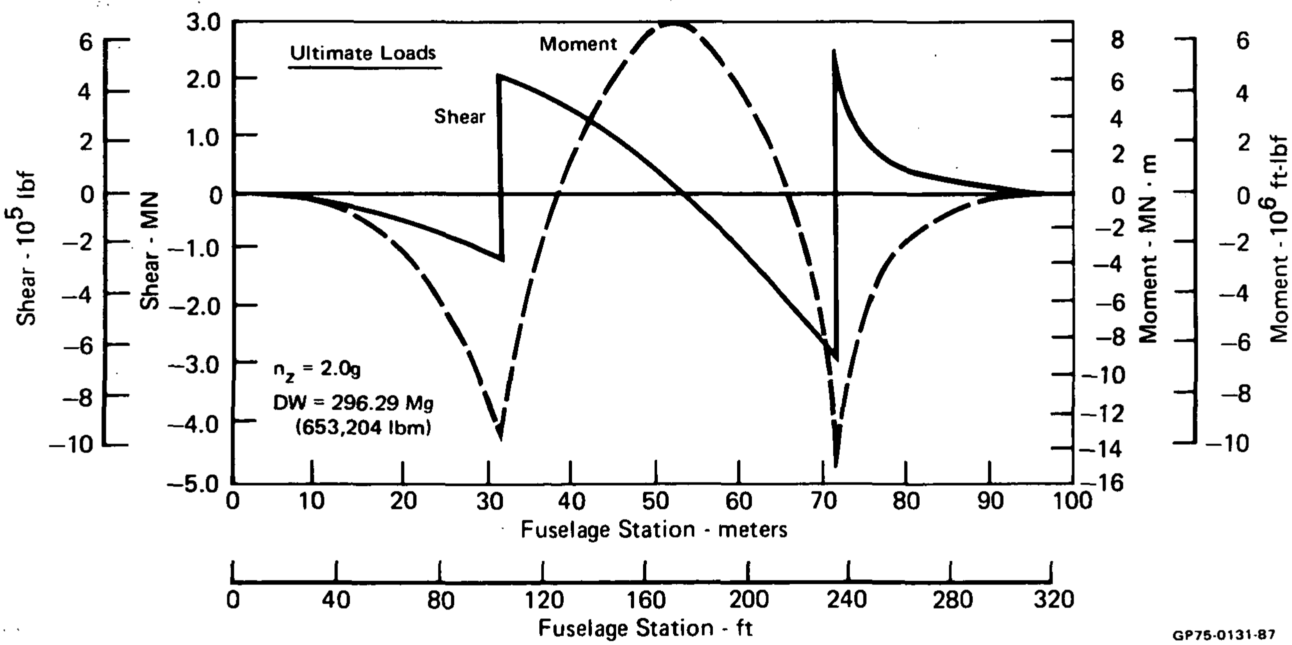

FIGURE 15
CONCEPT 3
Net Aircraft Shear and Moment
2g Taxi Condition

6. STRUCTURAL TRADE STUDIES

Structural definition of the three study Concept aircraft began with trade studies on volumetric efficiency, material utilization, and construction concepts to achieve maximum range for each conept. Section 6.1 sets forth aircraft sensitivities by which evaluation was made. Sections 6.2, 6.3, and 6.4 set forth the trade studies associated with each concept. Further discussion of these trade studies can be found in Section 6 of Reference (1).

6.1 RANGE SENSITIVITY

Figures 16 and 17 present sensitivities of Concept 1 and 2 and Concept 3, respectively, to weight and fuel quantity. These curves were derived from aerodynamics studies reported in Reference (1). They can be used to assess range change resulting from differences in structural concept. A structural growth factor of 9% was assigned to these aircraft to account for modification of structural components such as wings and landing gear. The curves are used in the following manner: (1) for dead weight changes multiply ΔOWE by 1.09.

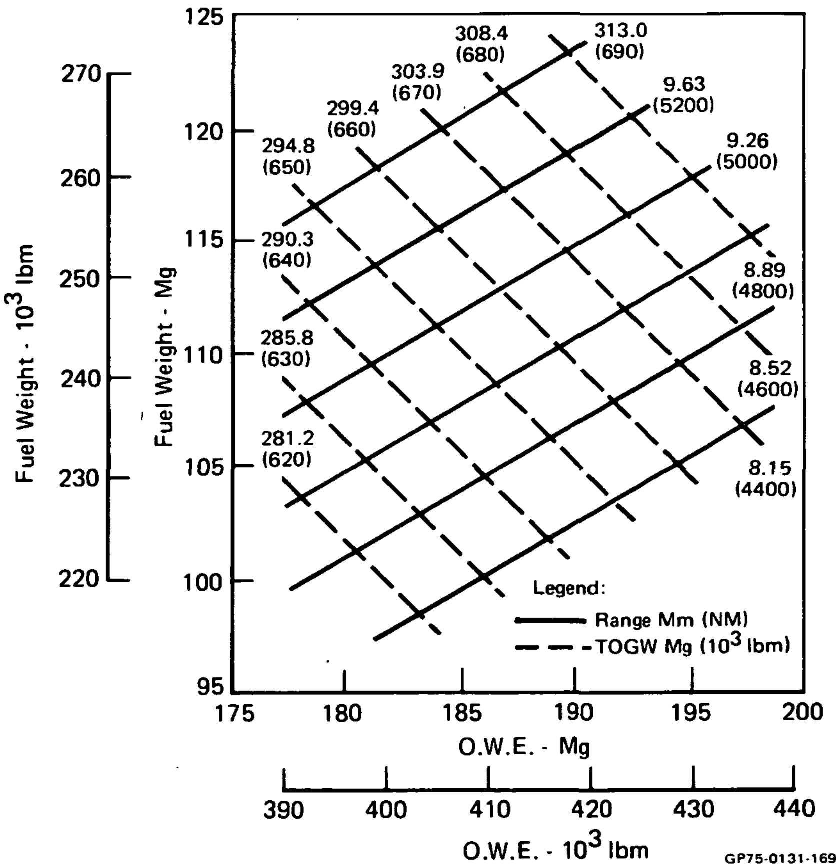

FIGURE 16
RANGE SENSITIVITY, CONCEPTS 1 AND 2

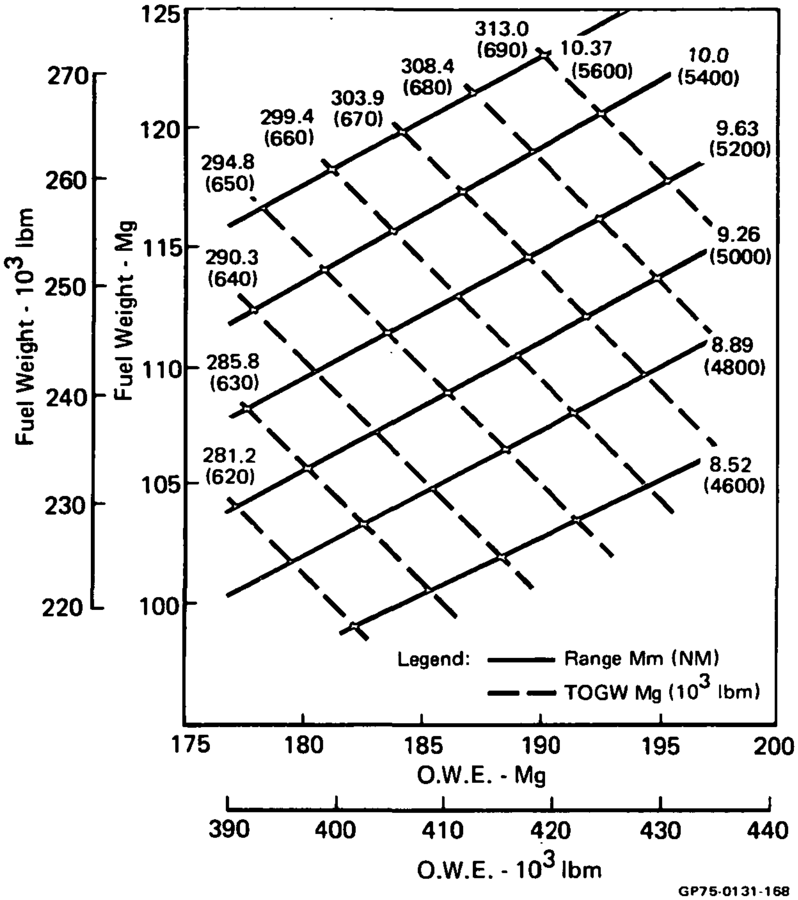

FIGURE 17
RANGE SENSITIVITY, CONCEPT 3

Enter the chart at old OWE + 1.09 ΔOWE; (2) for a change in total fuel weight multiply Δfuel weight by 0.09 to obtain the ΔOWE. Enter the chart with the old fuel weight + Δfuel weight and the old OWE + 0.09 Δfuel weight; (3) for changes in both OWE and total fuel weight perform steps 1 and 2 combined.

6.2 CONCEPT 1 TRADE STUDIES

Trade studies conducted for the Concept 1 aircraft affected not only construction of the fuselage shell but configuration and design philosophy of the non-integral tanks as well. A summary of these trade studies can be found in Reference (1).

6.2.1 Fail-Safe Versus Safe-Life Tanks - Fail-safe designs were considered but were discarded, since they would involve concepts such as double-walled tanks and would be considerably heavier. Accordingly, an all-welded safe-life concept was adopted for this study, and included in the fracture mechanics analysis of the tanks. Fail-safe and safe-life definitions are included in the structural design criteria presented in Section 3.

6.2.2 Tank Length and Dome Shape Studies - These studies and the passenger compartment location study discussed in Reference (1) illustrated the impact of volumetric efficiency on performance of the study aircraft. Figure 18 summarizes the combined effects of tank length and dome shape on range, based on the resulting tank weight and available fuel quantities. Range sensitivity to the calculated quantities is taken from Figure 16. The trend is clear. The least number of tanks (maximum length) and elliptical dome shape results in maximum aircraft range.

	Elliptical Domes	Hemispherical Domes	Torispherical Domes
2 Tanks	0 Selected	−233 (−126)	−128 (−69)
3 Tanks	−204 (−110)	−557 (−301)	−406 (−219)
4 Tanks	−520 (−281)	−976* (−527)	−769* (−415)

*Approximate - Based on Extrapolated Sensitivity

GP75-0131-90

FIGURE 18
NON-INTEGRAL TANK TRADE STUDY RESULTS
Basis: Δ Range - km (NM)

That trend is not shown in a comparison where only structural efficiency for containment of fuel is considered. Figure 19 presents structural efficiency (weight of fuel contained/weight of containment structure) as a function of the weight of fuel contained. This shows that the maximum number of fuel tanks with hemispheric domes yields maximum structural efficiency for low fuel quantities. At realistic takeoff fuel quantities Figure 19 results agree with Figure 18 wherein range is the figure of merit. Efficiencies presented in Figure 19 were based on a fixed size cylindrical envelope. Radial clearance was allowed between the tank and wall and the inside of the structure to accommodate insulation, tank deflection under load, tolerances, and a nominal gap. Deflection calculations were considered important since shorter tanks, which

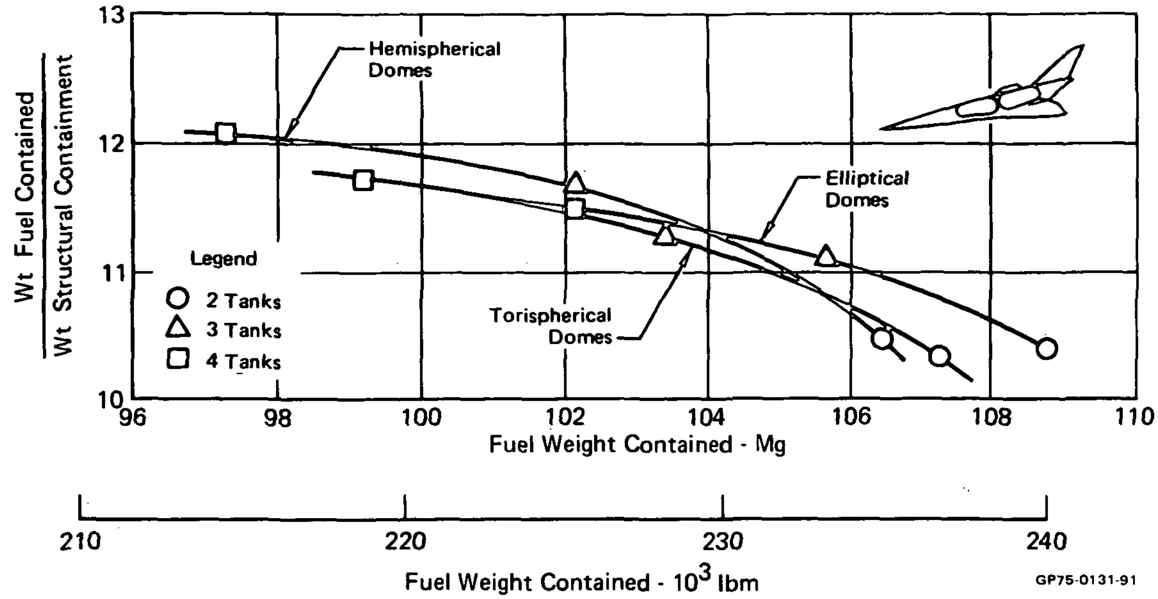

FIGURE 19
NON-INTEGRAL FUEL TANK WEIGHT AND VOLUME TRENDS

do not deflect as much as longer ones, were increased in diameter to fill the envelope. The tanks were considered to be welded 2219 aluminum construction with full monocoque walls. Each tank was found to be fully designed by the burst pressure condition and showed adequate margins of safety for all other design conditions.

Elements included in the weight calculations for this study included the tank shell, rings, internal redistribution members, fittings, weld lands, support links, and material added to the fuselage for tank load redistribution. Fuel system weights and allowances for construction details, such as manholes for inspection and services, were included.

A single tank concept was not considered for this study since preliminary analysis had shown such a configuration to be non-competitive in terms of weight. The single, full-length tank would have added only minimal fuel, since its diameter would have to decreased to meet the deflection criteria. Integral tank wall stiffening, added to accommodate bending would have not only added considerable weight to the fuel containment structure but would not have been directly comparable in cost to the monocoque skin constructions.

The effect of dome shape was also studied. Figure 20 tabulates volumetric efficiency and relative weight for each of the three dome shapes which came under final consideration. The basis for weight comparison is a membrane hemispherical head with a weight equal to $\pi \rho PR^3/F_{TU}$. The volume baseline was taken to be that of a flat-ended cylinder with its length equal to its radius. Volume comparison was then made to that constant length tank segment. From the comparison made in Figure 20 it is clear that while weight differences are relatively small, elliptical domes have the highest efficiency. The effect on Concept 1 range is presented in Figure 21. The elliptical dome shape was selected for Concept 1 on the basis of the data presented here. This shape was also used on the Concept 2 and 3 tanks assuming that these trends would be valid.

The range effect of tank length alone is also presented for reference in Figure 22.

Shape	Weight / Weight of Baseline	Volumetric Efficiency
Elliptical (a/b = 1.4)	0.95	0.764
Hemisphere	1.00	0.667
Torispherical	0.93	0.704

Basis: Hemispherical dome weight = $\pi \rho PR^3/F_{tu}$

GP75-0131-92

FIGURE 20
VOLUMETRIC EFFICIENCY AND WEIGHT OF DOME SHAPES

Dome Shape	ΔRange km (NM)
Elliptical	0 (0)
Torispherical	−128 (−69)
Hemispherical	−233 (−126)

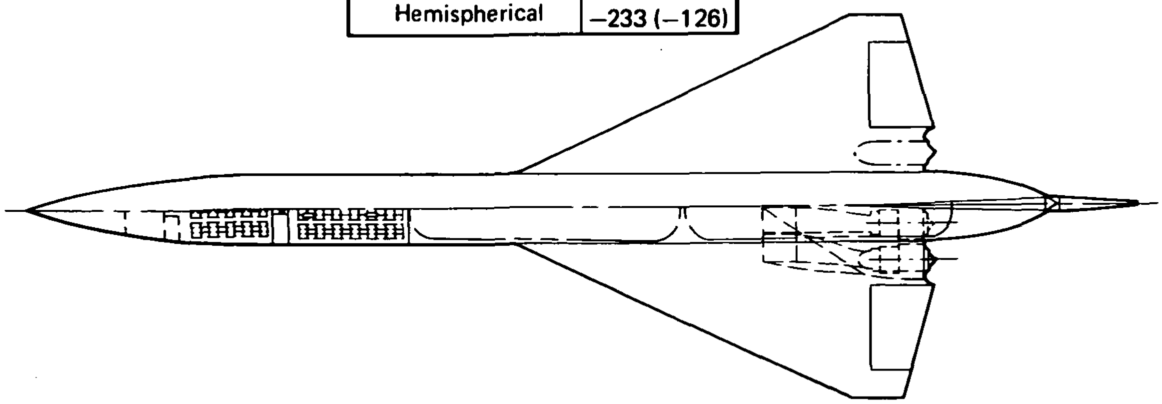

GP75-0131-93

FIGURE 21
RESULTS-FUEL TANK DOME SHAPE STUDY: (2 TANKS)

Number of Tanks	ΔRange km (NM)
2	0 (0)
3	−204 (−110)
4	−520 (−281)

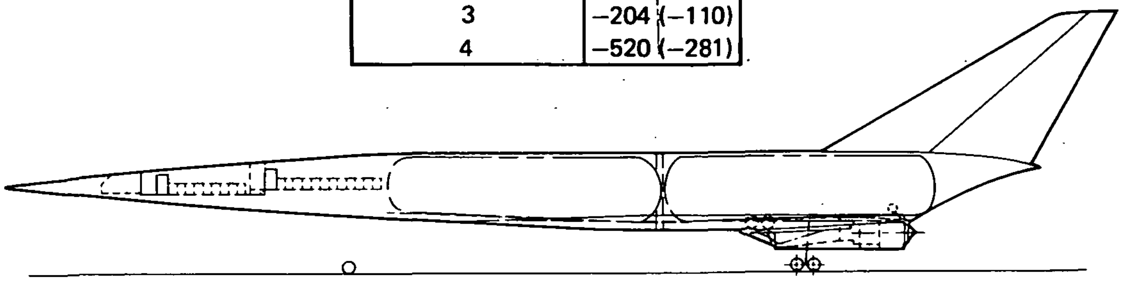

GP75-0131-94

FIGURE 22
RESULTS-FUEL TANK LENGTH STUDY: (ELLIPTICAL DOMES)

6.2.3 Tank Construction Study - Integral stiffening schemes were initially considered for the non-integral fuel tank. Strength analysis, based on the structural design criteria presented in Section 3 and the tank geometry described above, showed stiffening not to be necessary. Once burst pressure analysis set tank thickness the tank had adequate margins of safety in bending for the emergency landing condition and good margins of safety for all other conditions. The crash condition produced the maximum bending moments in the simply supported tanks. None of the integral stiffening concepts considered (Isogrid, 0-90° waffles) were able to show an advantage over pure monocoque shells. An Isogrid tank wall for instance would add approximately 45.4 kg (100 lbm) to the aircraft and result in a loss of nearly 3.7 km (2 NM) in range. Therefore, a monocoque shell was selected for the non-integral Concept 1 tankage.

6.2.4 Actively Cooled Fuselage Covering Study - Actively cooled panels of both honeycomb and beaded construction were compared to determine the most favorable covering for Concept 1. The critical failure mode for these panels was compressive buckling. For that reason flat panel edgewise compression buckling analyses were conducted. Coolant tubes were spaced on the basis of a heating rate of 68.1 kW/m^2 (6 $Btu/Sec\text{-}Ft^2$) for all panels with the temperature gradient set at 56 K (100°F) maximum. Thermal stresses were not taken into account because analysis conducted previously on the Actively Cooled Panel Program, Reference (8) showed thermal stresses resulting from the 56 K

(100°F) gradient to have a negligible effect on panel general stability. Analysis conducted for this study considered 2219-T87 material at an average temperature of 366 K (200°F) and used the load range within which the Concept 1 aircraft operates. Results of the panel construction comparison can be seen in Figure 23.

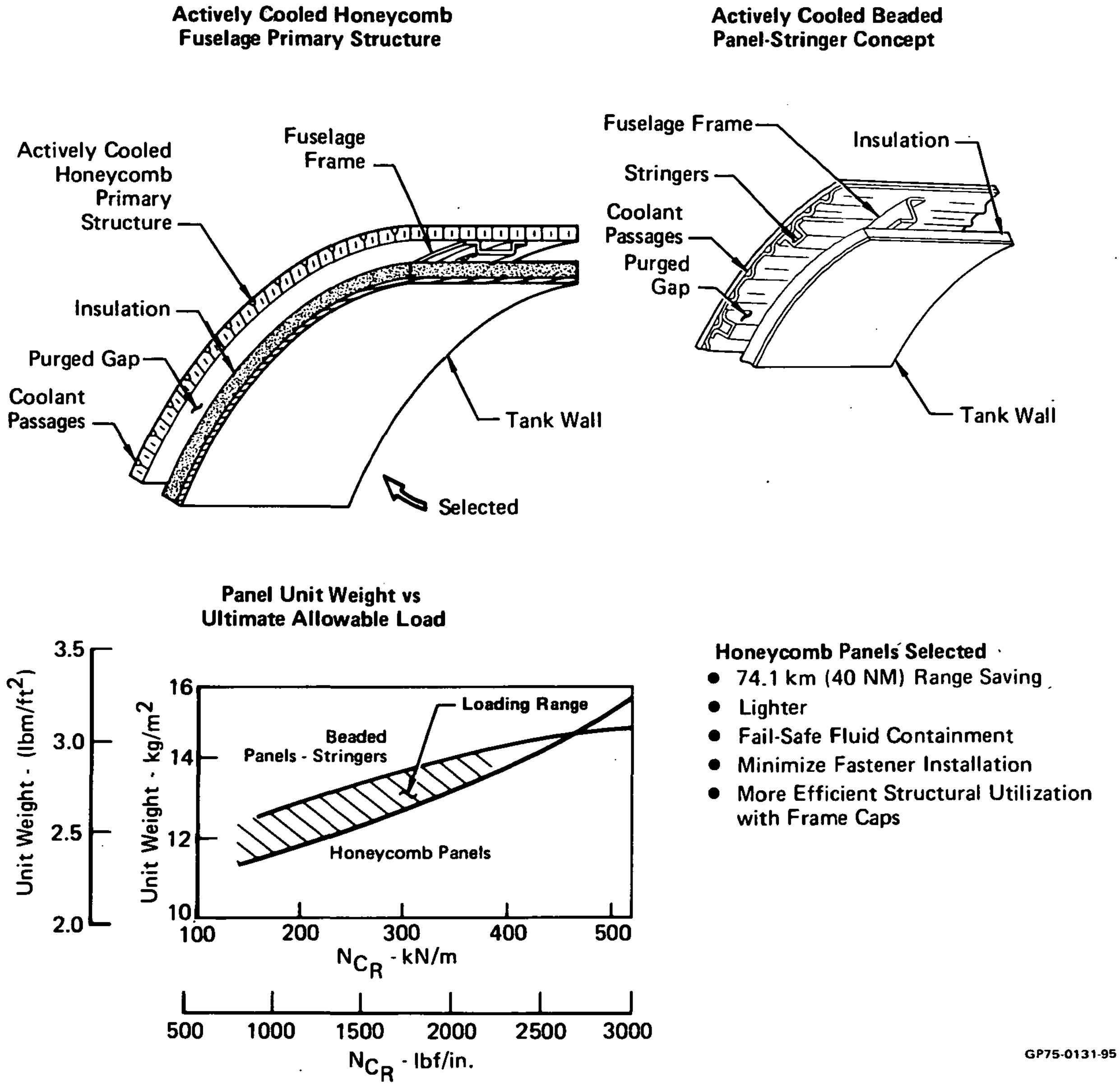

FIGURE 23
PRIMARY STRUCTURAL COVERING SELECTED

The honeycomb panels utilized 8.64 mm (0.34 in.) inner diameter, 0.89 mm (0.035 in.) wall "dee" shaped coolant tubes and the skins were limited to a minimum 0.635 mm (0.025 in.) thick outer face sheet and 0.406 mm (0.016 in.) thick inner face sheet. These skin thickness minimums were selected considering service damage and manufacturing handling. A 49.7 kg/m^3 (3.1 lbm/ft^3) honeycomb core was used to stabilize the face sheets and provide protection against coolant loss from a failed tube.

The beaded panel construction utilized 1.05 mm (0.040 in.) minimum thickness outer face sheets, 0.635 mm (0.025 in.) thick beaded panels bonded and riveted to the face sheet inside surface, and 1.02 mm (0.040 in.) thick hat section stiffeners, mechnically attached to the inner surface of the assembly.

Weights compared in Figure 23 include not only the load carrying structure but also splices, manifolds, shear clips, adhesives, fasteners, residual coolant, and an allowance for coolant pumping power.

The honeycomb construction panel was selected because it results in a lighter aircraft. The honeycomb panels provide fail-safe coolant containment in the event of tube failure, minimize the number of mechanical fasteners, and provide better flexibility in tailoring local load capability.

Subsequent calculations, based on final sizing of the Concept 1 fuselage/tank area covering, indicated that a weight penalty of 1.38 Mg (3050 lbm) would have been incurred by use of the beaded panel concept. This would have shortened Concept 1 range by 74.1 km (43 NM).

Weight penalties calculated for the 3.45 kPa (0.5 psi) gage purge pressure amounted to 44 kg (97 lbm). The effect on Concept 1 range is slight, 2.53 km (1.4 NM).

6.3 CONCEPT 2 TRADE STUDIES

Further trade studies were conducted on Concept 2 with the safe-life tank design philosophy, the two-compartment tank, and honeycomb construction actively cooled panels being retained from the Concept 1 studies.

6.3.1 Tank Construction Study - A monocoque tank shell could not be stabilized to carry the Concept 2 fuselage loads without the addition of stiffeners. Isogrid construction, with grid stiffening external, was selected for Concepts 2 and 3, rather than the 0°-90° waffles, because of the potential weight saving, illustrated by Figure 24. This method of construction also improves volumetric efficiency of the aircraft by minimizing the structural depth required for integral stiffening. A full discussion of the special features of Isogrid construction, as well as analysis methods used for this study, are found in Reference (9).

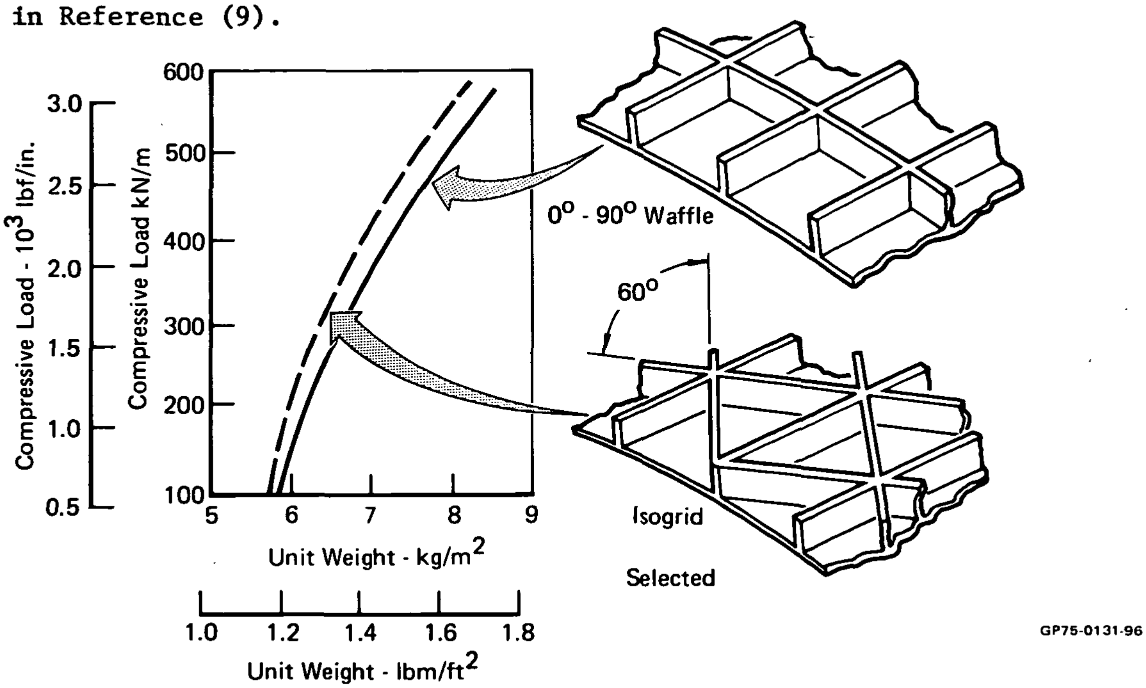

FIGURE 24
INTEGRAL TANK WALL CONSTRUCTION

In addition to the Isogrid and 0-90° waffles, three other methods of tank wall construction were considered for this study. The first was a 0-90° waffle pattern modified by the addition of discrete rings. These rings would also be used as supports for the actively cooled panels. Thermal gradients, however, from 20.3 K (-423°F) at the tank wall to 366 K (200°F) at the panel inner surface would create drastic thermal stress problems in a continuous ring. For this reason the continuous rings were eliminated from further consideration.

Integral stiffening by means of $\pm 45°$ waffle patterns and plain monocoque skin construction were also considered but were not competitive from a weight standpoint. On Concept 2, the waffle pattern would be 246 kg (542 lbm) heavier than an Isogrid tank and would penalize the aircraft slightly over 14.8 km (8 NM) in range.

6.3.2 Semi-Structural Versus Non-Structural Fuselage Covering Study - Since the integral tankage carries the primary aircraft structural loads, actively cooled panels in the integral tankage region could be expected to carry no primary loading. However, the minimum height panels weigh approximately 90% of the Concept 1 panels which were used in a structural configuration. Therefore, a trade study of the Concept 2 aircraft fuselage was conducted to compare strictly non-structural panels with semi-structural arrangement. The non-structural panels were assumed to be supported individually from the integral hydrogen tank and had slip joints around their periphery to allow relative motion between panels. In the semi-structural arrangement all the panels in the tank area were interconnected, and supported, on frames, from the upper wing surface.

The semi-structural version is illustrated in Figure 25. The arrangement is similar to that employed on Concept 1 except that a major slip-joint is utilized at each end of the cover. These slip-joints are designed to allow thermally induced motion between the tank and fuselage cover. Since the lower edge of the cover is continually connected to the wing carry-through, it must take the same deflected shape as the remainder of the fuselage, and bending loads are thus introduced. The maximum compressive running load in the semi-structural covering are only 87.6 kN/m (500 lbf/in.) or less than 20% of those for the primary structural covering on the Concept 1 aircraft. The minimum height, 1.27 cm (0.5 in.), panels did not have to be increased in weight to carry these loads. This semi-structural cover relieves the integral tank bending loads enough to reduce the tank shell weight by approximately 998 Kg (2,200 lbm). Range sensitivity curves for the Concept 2 aircraft equate this weight saving to a range gain of nearly 57 km (31 NM). Thus the semi-structural arrangement was chosen for the covering on Concept 2.

The effect of the 3.45 kPa (0.5 psi) gage purge pressure on the fuselage covering is approximately the same as reported for the Concept 1 aircraft in Section 6.2.4.

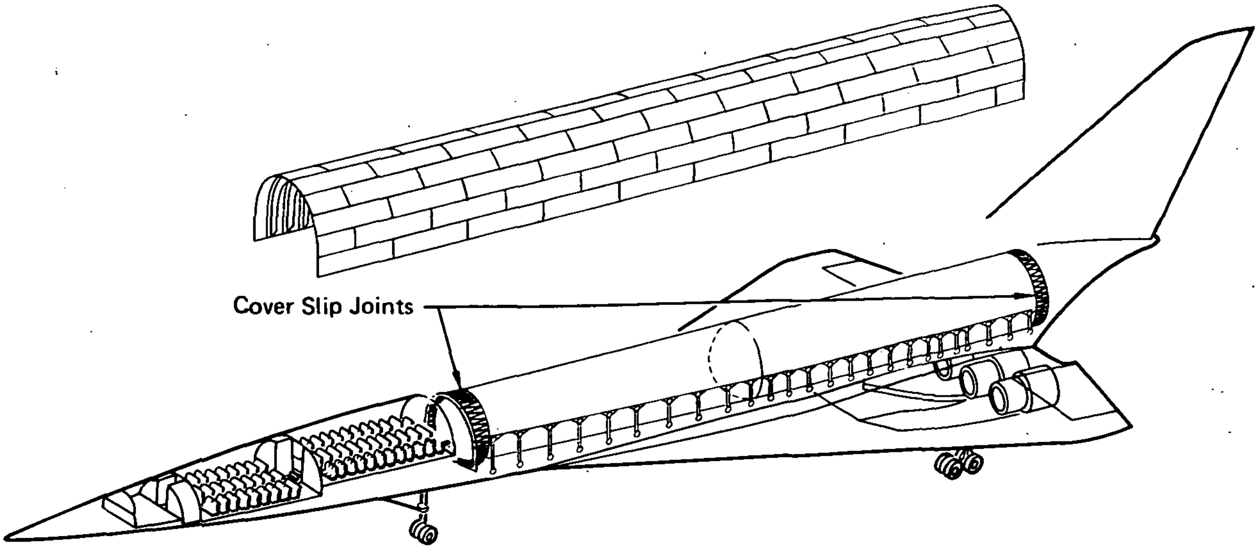

FIGURE 25
SEMI-STRUCTURAL FUSELAGE COVERING

6.4 CONCEPT 3 TRADE STUDIES

The Concept 3 fuselage/tank area retained a number of the features of Concepts 1 and 2. Those were the safe-life tank design, the two-compartment tank, and the actively cooled panel construction. The Isogrid tank wall construction selected for Concept 2 was found to be applicable to Concept 3. It was necessary, however, to reconsider the semi-structural fuselage covering and establish the most efficient tank cross section. Those studies are reported below.

6.4.1 Semi-Structural Vs Non-Structural Fuselage Covering Study - Preliminary investigation revealed that a semi-structural arrangement for actively cooled panels would either induce excessive thermal stresses or require such large frames that aircraft range would be degraded. Potentially, the weight saving in the Concept 3 multi-bubble tank would be mostly in the centerline bubble, but it would be much smaller than the Concept 2 savings. (See Section 6.3.2)

It was, therefore, decided to eliminate the semi-structural cover from further consideration. The only loading imposed upon these chosen non-structural panels is airload and purge pressures. The panels are supported from the tank by a linkage arrangement that is capable of transmitting the airloads to the primary structure without inducing thermal stresses into the panels.

The panels are at a minimum practical fabrication thickness of 12.7 mm (0.5 in.). At that thickness, and using the panel support scheme indicated in Figure 44 of Reference (1), the panels are adequate to accept the 3.54 kPa (0.5 psi) purge pressure, in addition to the normal airloads pressures, without weight or range penalty.

6.4.2 Tank Cross Section Optimization - The study contract statement of work, Reference (3), recognized the need for a multi-bubble cross section in the fuel tanks to attain maximum volume utilization in the blended-body fuselage. The optimization task, then, was to determine the number of bubbles in the cross section which will maximize aircraft range.

The first step was to determine weights for several tank configurations. When those results were transformed into a structural and volumetric efficiency, as indicated in Figure 26, only minimal gains result from increasing the number of bubbles above 5. The range penalty associated with a fixed tank length and changing tank cross section is presented in Figure 27. On the basis of this study a five-bubble cross section was selected for the Concept 3 fuel tanks.

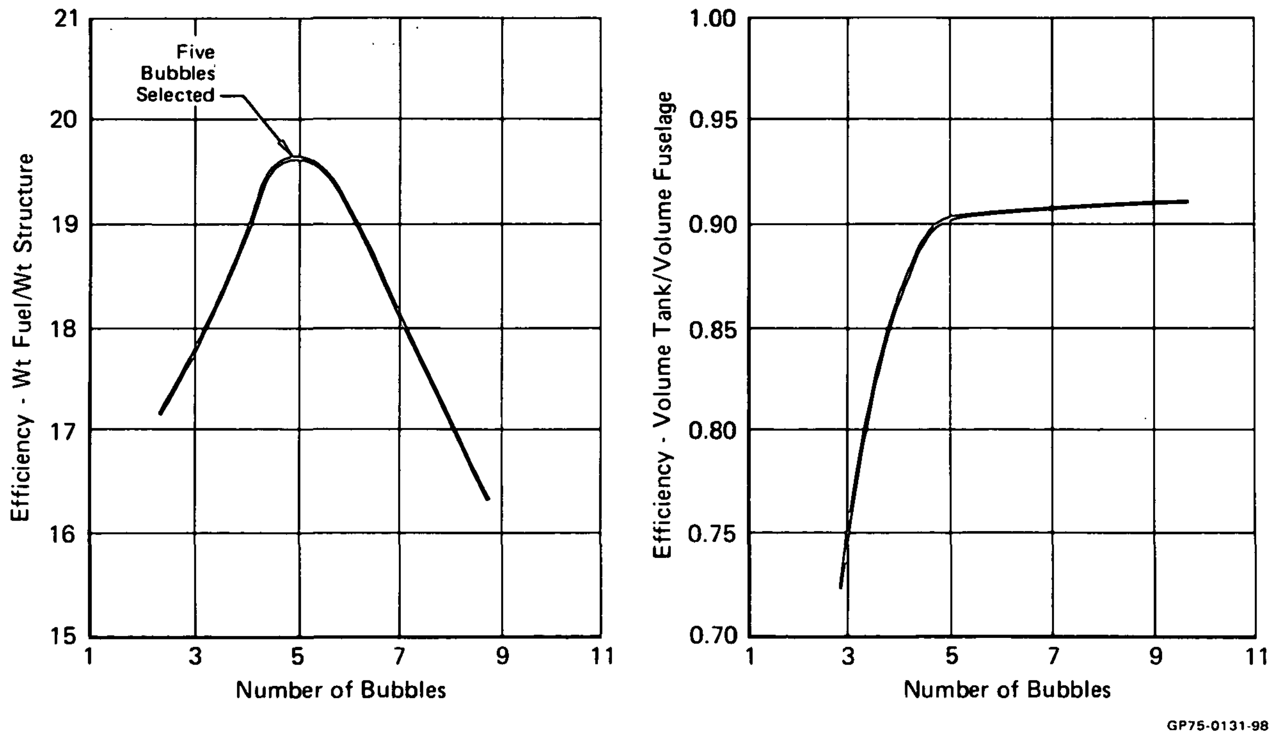

FIGURE 26
CONCEPT 3 - TANK CONFIGURATION TRADE

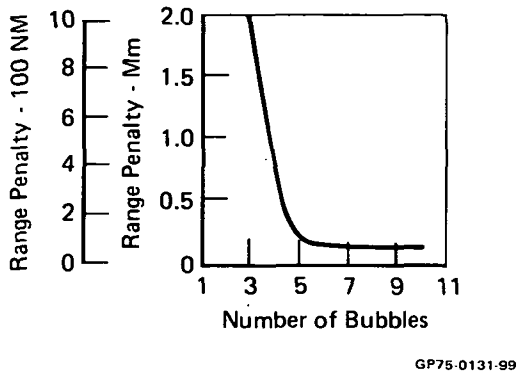

FIGURE 27
MULTI-BUBBLE TANK RANGE PENALTY

7. STRUCTURAL ANALYSIS FOR WEIGHT REFINEMENT

Volumetric efficiency, aerodynamic performance and aircraft weight are the three most important factors affecting range in this study. Volumetric efficiency and aerodynamic performance were discussed in Reference (1). Accurate evaluation of the fuselage/tank area structural weight was essential to a valid comparison of the three aircraft concepts being considered.

7.1 CONCEPT 1 WEIGHT REFINEMENT

After the Concept 1 aircraft had been initially sized to contain the payload, and the amount of fuel to attain the required mission range was determined, a finite element computer model was constructed which represented the fuselage/tank area structure. That model was then used to determine the magnitudes and distribution of the internal loads resulting from the external loads applied to the aircraft. These internal loads were then used for detailed sizing of representative structural components and for refinement of the center fuselage weights.

7.1.1 Finite Element Computer Model - The modeling process was started by generating the moldline geometry on the cathode ray tube (CRT) system which is an integral part of MCAIR's main computer complex. (It was necessary to create the model on only one side of the vertical centerline since the analysis program creates a mirror image on the other side.) Frames, bulkheads, cover skins, wing ribs, etc., were then modeled. Intersecting straight line elements were used to represent the curved surfaces of the aircraft as shown in Figure 28. Points were generated wherever two or more of the bar elements met. The resulting complex is called a "Point-Line" model.

That model was then transformed into the required finite element structural model by transforming the points to joints, the lines to bars, and adding shear panels. The model then represents the actual aircraft structure.

The model created for Concept 1 was simplified by spacing the fuselage frames at approximately 3.05m (10 ft) intervals instead of the approximate 0.91m (3 ft) spacing on the aircraft. Proper stiffness simulation of these frames was attained by using the "lumped" area of the three aircraft frames in the single model frame with the proper modulus of elasticity. This was done on all three models to reduce the number of modeled structural components and the cost of computer aided analysis. It is felt that the depth of

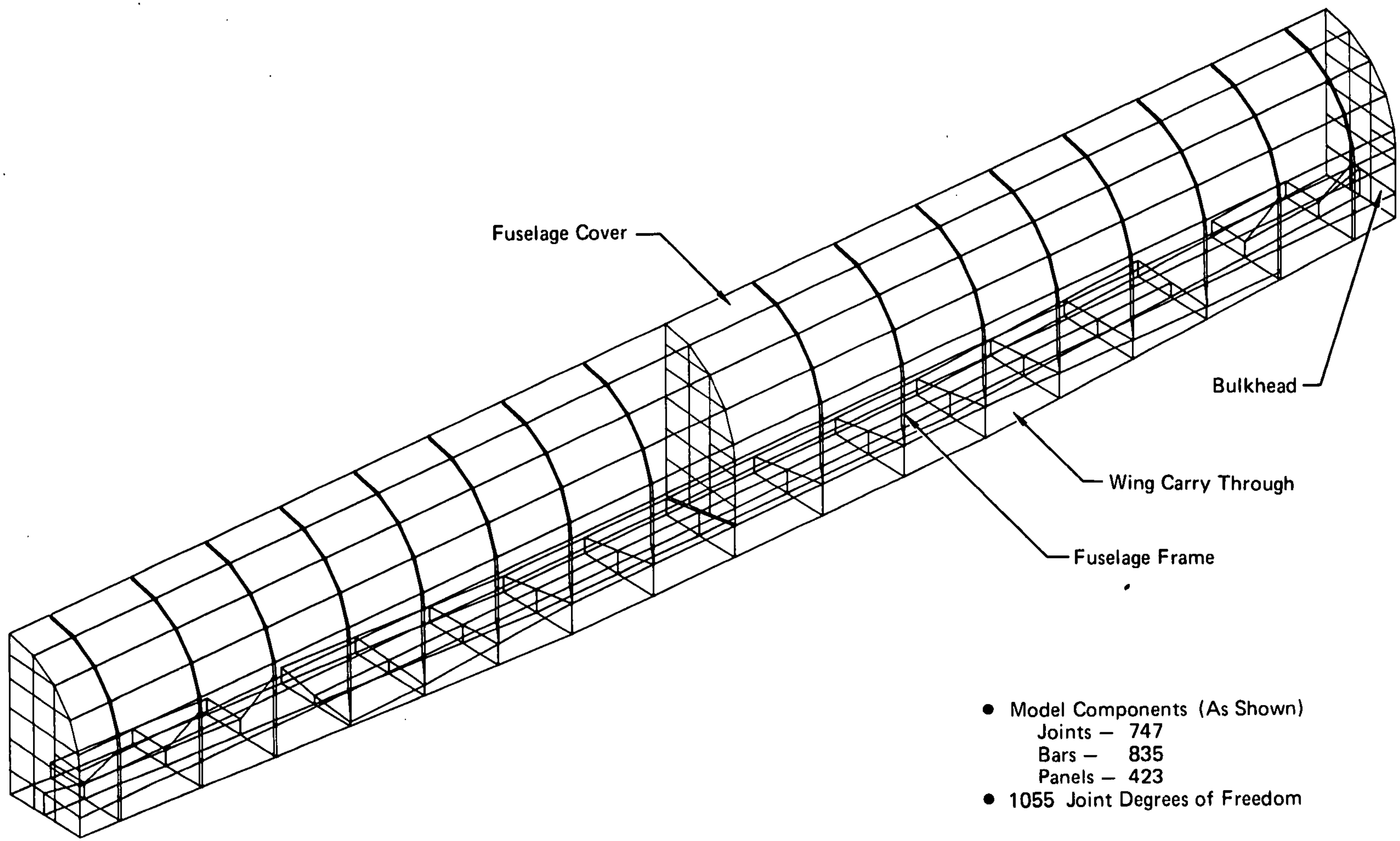

- Model Components (As Shown)
  - Joints – 747
  - Bars – 835
  - Panels – 423
- 1055 Joint Degrees of Freedom

GP75-0131-100

FIGURE 28
CONCEPT 1 - FINITE ELEMENT COMPUTER MODEL
Fuselage/Tank Area

analysis is adequate to disclose the relative weight and range differences of the three concepts.

The finite element model of the fuselage/tank area of Concept 1 is illustrated in Figure 28. The wing carry-through, structural fuselage cover, and fuselage frames and bulkheads can be readily identified. The number of joints, bars, panels and joint degrees of freedom for the half model are listed on Figure 28. Stiffness constraints from structure external to the center fuselage were ignored.

7.1.2 Input Load Vectors - Aircraft loads presented in Section 5 were used to define the input vectors to the computer analysis program. The appropriate bending moments and shears were applied to the ends of the model and the combination of airload and inertia as well as wing root moment and shear were applied at each fuselage station former. Since both loading conditions are symmetrical, loads for one side only are presented here.

a. End Load Introduction - A typical conversion of end moments and shears into input vectors is shown in Figure 29. Two items are worthy of note. The first is that vectors A and K are only half of the magnitude that might be expected. Because of their position on the model centerline of symmetry, the same load is duplicated on the mirror image side of the model during the analysis run so only one half of the load is inputted. The other

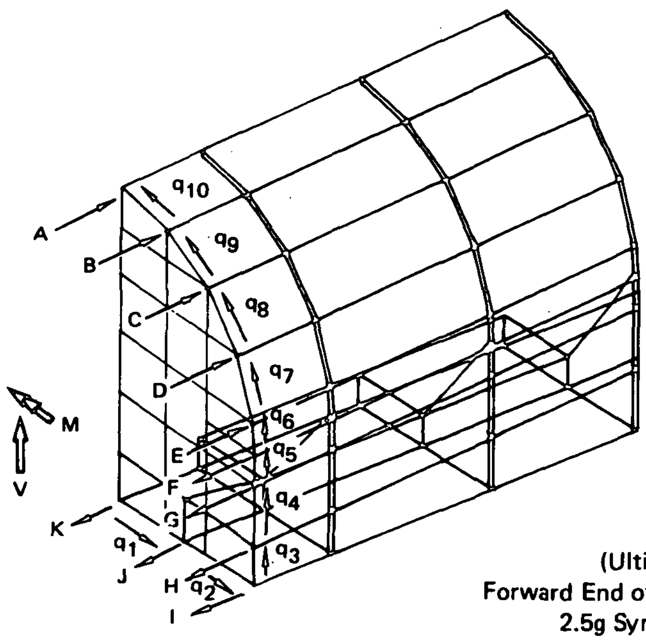

	Axial Vectors			Bar Loads	
	kN	(10^3 lbf)		N	(lbf)
A	157.1	(35.32)	q_1	169.0	(38)
B	292.2	(65.68)	q_2	618.3	(139)
C	236.4	(53.14)	q_3	934.1	(210)
D	151.3	(34.02)	q_4	1143.2	(257)
E	47.0	(10.56)	q_5	613.9	(138)
F	8.5	(1.92)	q_6	605.0	(136)
G	64.8	(14.56)	q_7	1121.0	(252)
H	177.0	(39.78)	q_8	547.1	(123)
I	247.1	(55.55)	q_9	489.3	(110)
J	256.0	(57.54)	q_{10}	1574.7	(354)
K	130.6	(29.36)			

M = 9.02 MN · m (6.65×10^6 ft-lbf)

V = 8.90 kN (2×10^3 lbf)

(Ultimate Loads)
Forward End of Fuselage/Tank Section
2.5g Symmetrical Pullup

GP75-0131-101

FIGURE 29
TYPICAL END LOAD INTRODUCTION, CONCEPT 1

is that shear flows have been converted into bar loads instead of the more normal joint load vectors. The bar load capability allows a more even and realistic distribution of load reaction.

b. Non-integral Tank Reactions - The Concept 1 non-integral tanks were not modeled for the finite element representation but were analyzed separately. Figure 30 illustrates the input loading vectors which were used to introduce the reactions from the forward tank into the primary structure. A similar set was used for the aft tank reactions.

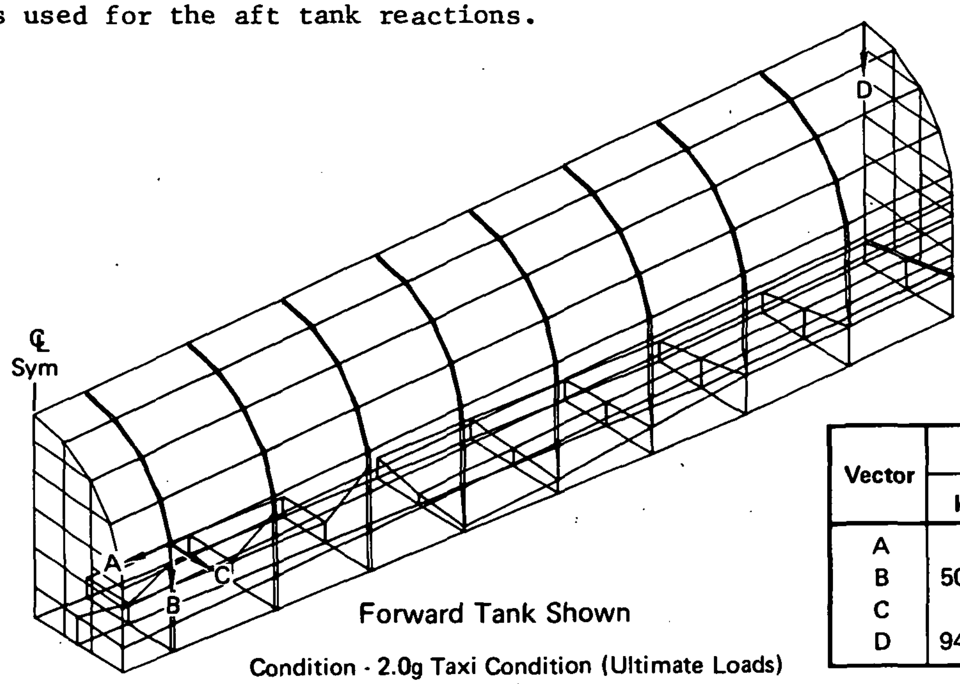

Vector	Magnitude	
	kN	(10^3 lbf)
A	0	0
B	502.9	113.06
C	0	0
D	943.3	212.06

GP75-0131-102

FIGURE 30
NON-INTEGRAL TANK REACTIONS - CONCEPT 1 AIRCRAFT

c. Typical Frame Loading - Each frame in the computer model had applied to it a set of in-plane loadings which represented local airloads, inertia, and wing root loading. A set of load vectors applied to a typical fuselage station former is presented in Figure 31. Vectors A, B and C represent the combination of fuselage and wing inertia and airload. In obtaining these loads it was assumed that lift on the fuselage consisted of positive pressure on the wing lower surface. Wing box inertia and fuselage lift over the fuselage length represented by the frame were then split into 5 vectors. This procedure determined the magnitude of vectors A and B with consideration of the fact that a force applied at the model centerline is duplicated during the analysis run. Vector C then was modified by algebraic addition of

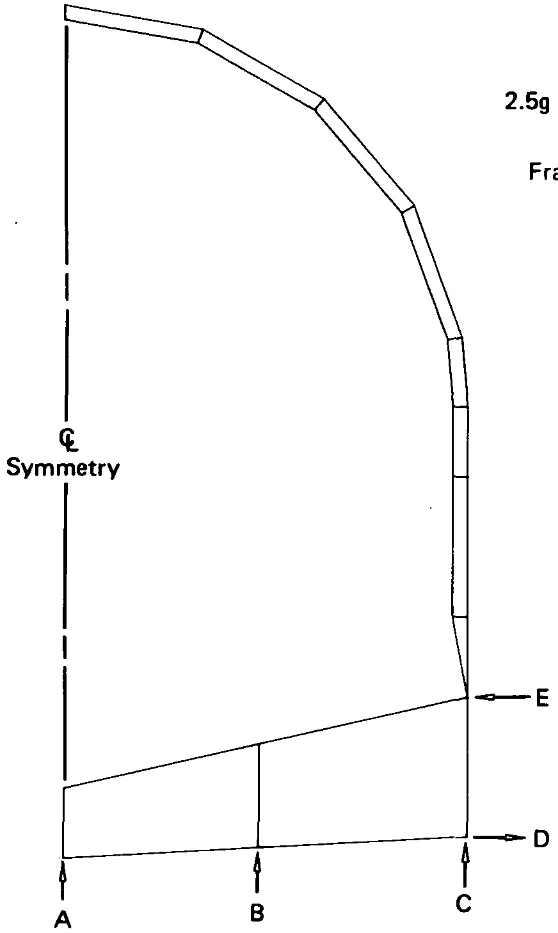

Vector	Magnitude	
	kN	(10^3 lbf)
A	5.1	1.16
B	9.8	2.20
C	254.4	57.20
D	951.0	213.80
E	951.0	213.80

GP75-0131-103

FIGURE 31
TYPICAL CONCEPT 1 FRAME LOADING

appropriate net wing load (lift less inertia) and the inertia of the fuselage cover. Vectors D and E represent the net wing root bending moment resulting from both airloads and inertia.

7.1.3 Finite Element Computer Analysis - The CASD (Computer Aided Structural Design) computer program was used with the finite element models and input loading discussed above to determine structural member sizing and internal load distributions in the aircraft. An estimated nominal size as well as a minimum size for each member was also entered, along with allowable tension, compression and shear stress and modulus of elasticity. Once all of the input data had been recorded, the program then calculated a stiffness matrix and internal loads for each input loading condition.

A resizing routine was used with all of the runs made for this study. This routine uses the input allowable stresses, areas, thicknesses and calculated internal loads to compute margins of safety on each element, and the element is resized to obtain a margin of safety closer to the desired zero value. The resizing was accomplished on the basis of the most critical of the two input loading conditions, either the 2.5g symmetrical pullup or the 2.0g taxi condition.

A new stiffness matrix, revised internal loads and new margins of safety were then generated. Three cycles of this process were used to determine final internal loading for the study aircraft.

7.1.4 Detailed Analysis of Representative Components - In addition to element sizing, the CASD program provided bar axial loads and shear panel loads which were available to the analyst either on the CRT or in printed form. These loads were used for detailed strength analysis of the structural members. Figure 32 presents a stability analysis of one of the actively cooled panels. This analysis was repeated in several areas over the surface of the fuselage and the results used in weight refinement.

The non-integral fuel tank was analyzed by conventional methods. As seen in Figure 33, the tank skin thickness was first determined by design burst pressure. The subsequent buckling analysis of the crash condition showed the pressure stabilized tank to have an adequate margin of safety. A larger margin of safety would be evident for the 2.5g flight condition. The thicknesses calculated for the tank burst pressure requirement, together with estimated ring and stiffening weights, were thus used to generate the tank weights.

7.1.5 Structural Weight Refinement - Results of the weight refinement process on Concept 1 are compared to the statistical weight estimate in Figure 34. The most significant changes were in the area of the monocoque structural shell where the actively cooled panels were 2.2 Mg (4850 lbm) heavier than originally estimated, but the frame and bulkhead weight beneath them was 3.97 Mg (8473 lbm) lighter, largely as a result of the use of the actively cooled panels as part of the frame caps. Total center fuselage weight estimation in this instance was shown to be only 1.5% in error.

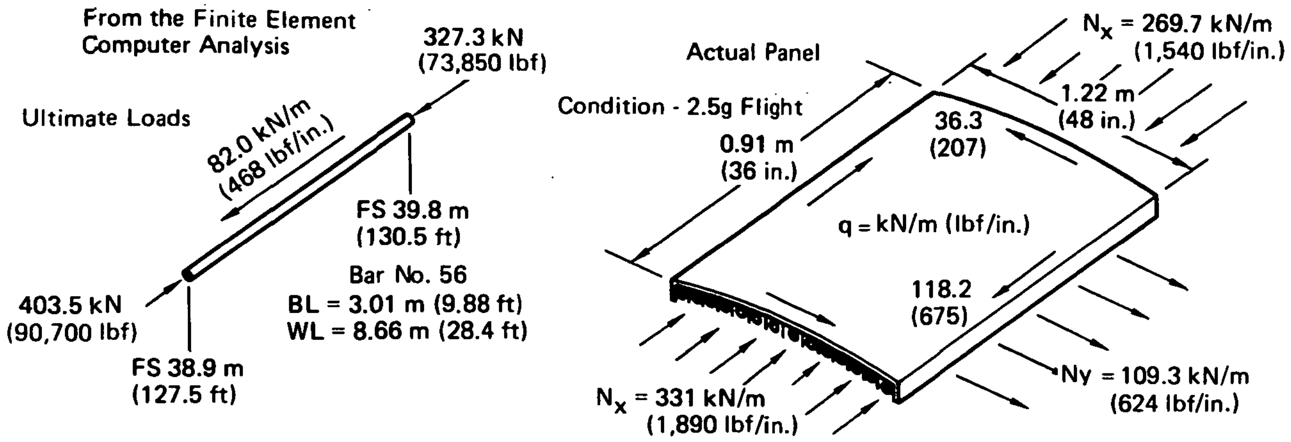

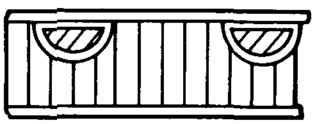

Panel Temperature = 396 K (200°F)

Panel Geometry

Panel Depth = 4.06 cm (1.60 in.)
Outer Skin t = 0.11 cm (0.045 in.)
Inner Skin t = 0.041 cm (0.016 in.)

Tube Dimensions:	
Wall t	= 0.089 cm (0.035 in.)
Inner Dia	= 0.86 cm (0.34 in.)
Spacing	= 5.08 cm (2.0 in.)

$A = 2.0\ \text{cm}^2/\text{m}\ (0.079\ \text{in.}^2/\text{in.})$

$D = EI = 878.2\ \text{N}\cdot\text{m}^2\ (30.6 \times 10^4\ \text{lbf/in.}^2)$

Neglecting the Stabilizing Effect of Curvature and Internal Pressure

All Equations and Constants
Taken from Reference 10

$$\text{Compression: } N_x cr = \frac{K_c \pi^2 D}{b_1^2} = 344.9\ \text{kN/m (1,968 lbf/in.)}$$

$$b_1 = 1.22\ \text{m (48 in.)}, k_c = 1.5$$

$$R_c = \frac{N_{x_{avg}}}{N_{x_{cr}}} = \frac{300.4}{344.9} = 0.871$$

$$\text{Shear: } N_{s_{cr}} = \frac{K_s \pi^2 D}{b_2^2} = 320.5\ \text{kN/m (1,830 lbf/in.) (Corrected for Plasticity)}$$

$$b_2 = 0.914\ \text{m (36 in.)}, k_s = 2.8$$

$$R_s = \frac{N_{s_{avg}}}{N_{s_{cr}}} = \frac{77.3}{320.5} = 0.241$$

$$MS = \frac{2}{R_c + \sqrt{R_c^2 + 4R_s^2}} - 1 = \frac{2}{0.871 + \sqrt{0.871^2 + 4 \times 0.241^2}} - 1 = +0.07$$

Panel Weight:	kg/m^2	(lbm/ft^2)
Skins	4.37	(0.896)
Tubes	1.15	(0.235)
Manifolds	0.87	(0.179)
Core	2.51	(0.513)
Other *	4.43	(0.908)
Total	13.33	(2.731)

* Fasteners, Inserts, Splice Straps, Adhesive, Etc.

GP75-0131-167

FIGURE 32
ACTIVELY COOLED PANEL BUCKLING ANALYSIS, CONCEPT 1

Burst Pressure Analysis

Maximum Radius = 3.20 m (126 in.)

Factor of Safety = 2.0 (Section 3)
Pressure = 138 kPa (20 psi) Gage (Section 3)
Temperature = 294 K (70°F)

From Figure 10:

F_{tu} = 434.4 MPa (63 x 10^3 psi) Parent Material
= 193.1 MPa (28 x 10^3 psi) As-Welded

Thickness Required = $t_{reqd} = \frac{pR}{F_{tu}}$ x Factor of Safety
= 0.203 cm (0.080 in.) Parent Material
= 0.457 cm (0.180 in.) As-Welded

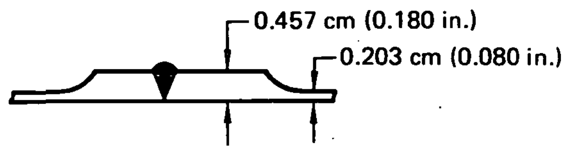

Bending Analysis

Crash Condition $n_z = 4.5$

Temperature = 20.3 K (–423°F)

Calculated Maximum Bending Moment (Ultimate) = 8.72 MN · m (77.22 x 10^6 in.-lbf)
Local Radius at Maximum Moment = 3.162 m (124.5 in.)
Bending Stress = $f_b = M/\pi R^2 t$ = 136.5 MPa (19.8 x 10^3 psi) - Parent Material
Limit Pressure Relief Stress = $f_p = pR/2t$ = 107.3 MPa (15.56 x 10^3 psi) - Parent Material
Maximum Tensile Stress = f_t = 243.8 MPa (35.36 x 10^3 psi) Ultimate - Parent Material
In the As-Welded Material the Fatigue M.S. = (0.203/0.457 x 243.8 ÷ 165) –1 = +0.34
Maximum Compressive Stress = f_c = 29.23 MPa (4240 psi)
From Reference 11, Figure C8.13a with L = 26.8 m (88 ft)
L/R = 8.48, R/t = 1556, $F_{bcr}/E = 5.9 \times 10^{-5}$, F_{bcr} = 4.88 MPa (708 psi)
Accounting for Pressure Stabilization from Reference 11, Figure C8.14

$$\frac{P}{E}\left(\frac{R}{t}\right)^2 = 4.035, \text{ Using the 90\% Probability Curve } \frac{\Delta F_{bcr}}{E} \times \frac{R}{t} = 0.5$$

$\therefore \Delta F_{bcr}$ = 26.58 MPa (3855 psi)

The Critical Bending Stress is Then: F_{bcr} = 31.46 MPa (4563 psi)

$$\text{M.S.} = \frac{31.46 - 29.23}{136.5} = +0.016$$ (A 1.6% Increase in Load Factor Would Fail the Tank)

2.5g Flight Condition

Maximum Bending Moment Becomes: $\frac{2.5 \times 1.5}{4.5} \times 8.72$ = 7.27 MN · m (64.32 x 10^6 in.-lbf)

Maximum Bending Stress = f_b = 113.7 MPa (16.5 x 10^3 psi)
Maximum Tensile Stress = f_t = 221 MPa (32.06 x 10^3 psi)
Maximum Compressive Stress = f_c = 6.4 MPa (930 psi)

Crash Condition Burst Pressure 160 kPa (24.4 psi)
Not Critical

$$\text{Bending M.S.} = \frac{31.46 - 6.4}{113.7} = +0.22$$

GP75-0131-174

FIGURE 33
NON–INTEGRAL FUEL TANK ANALYSIS

Center Fuselage	Original Weight Estimate Mg (lbm)	Refined Weight Estimate from Detail Calculations Mg (lbm)	ΔO.W.E. Mg (lbm)
1. Actively Cooled Panels	8.70 (19,185)	10.90 (24,035)	
2. Frames and Bulkheads	7.18 (15,823)	3.33 (7,350)	
3. Longerons	2.28 (5,029)	2.18 (4,800)	
4. Fuel Tanks	7.09 (15,635)	7.12 (15,699)	
5. Tank Insulation	1.68 (3,699)	3.02 (6,650)	
6. Tank Supports	0.46 (1,020)	0.39 (854)	
7. Misc Access Doors, Supports, etc.	2.46 (5,425)	2.46 (5,425)	
Total	29.85 (65,816)	29.40 (64,813)	–0.45 (–1,003)

GP75-0131-106

FIGURE 34
STRUCTURAL WEIGHT REFINEMENTS, CONCEPT 1

7.2 CONCEPT 2 WEIGHT REFINEMENT

The Concept 2 aircraft was configured to carry the same payload and fuel quantity as Concept 1. The refinement process was thus identical. Differences in details such as the finite element computer model are discussed in the following paragraphs.

7.2.1 Finite Element Computer Model - The structural representation of the Concept 2 fuselage/tank area is shown in Figure 35. This was the largest model used in the program in terms of the number of elements. The fuselage structure is quite similar to that of Concept 1, as can be seen by comparison to Figure 28. The tank model is illustrated as being separated from the fuselage in Figure 35 but the CASD program connects these two substructures during the analysis. On Concept 2 the connection is made at the lower end of the tank connecting links shown as part of the tank substructure. This same model, with the structural fuselage cover removed, was utilized for trade study on the semistructural versus nonstructural fuselage covering described in Section 6.3.2.

7.2.2 Input Loading Vectors - The major differences in input loadings between Concept 1 and Concept 2 occur at the model ends and in the tank itself. Since the tank is the primary structure, end moments and shears must be applied to the tank ends as shown in Figure 36 instead of to the surrounding structure. A typical tank frame loading is shown in Figure 37. These loads consist entirely of tank and fuel inertia. Frame loadings on Concept 2 are quite similar to those shown in Figure 31 for Concept 1.

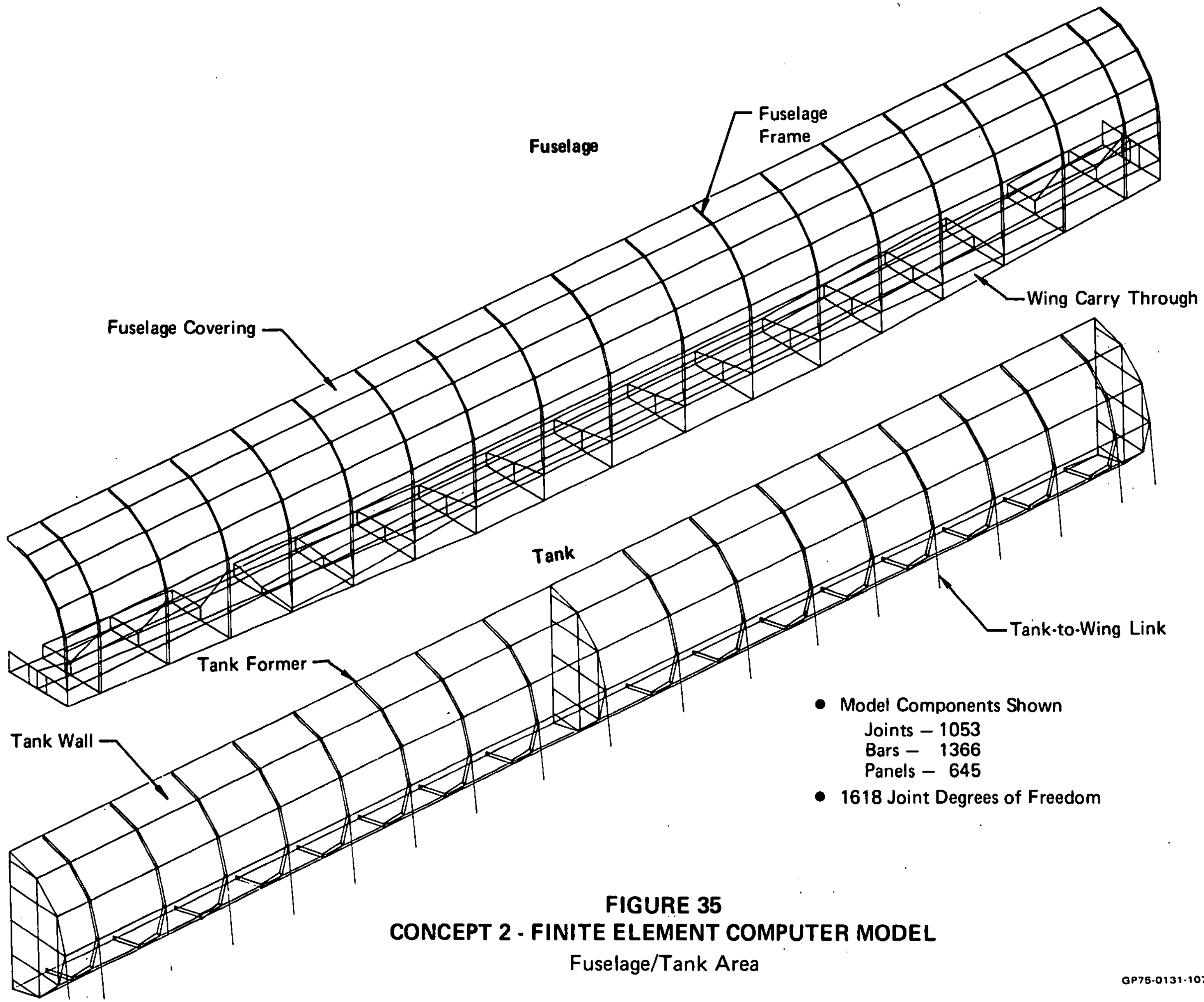

FIGURE 35
CONCEPT 2 - FINITE ELEMENT COMPUTER MODEL
Fuselage/Tank Area

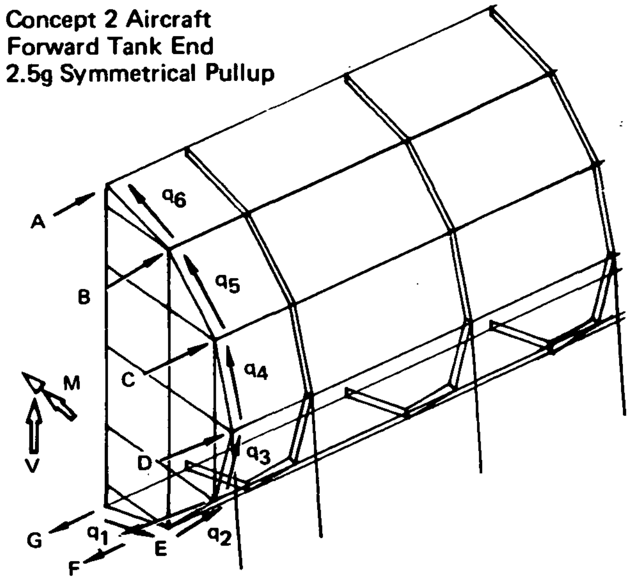

Axial Vectors kN (10^3 lbf)			Bar Loads N (lbf)		
A	231.9	(52.13)	q_1	876.3	(197)
B	401.7	(90.30)	q_2	2389.0	(537)
C	231.9	(52.13)	q_3	3265.0	(734)
D	0	(0)	q_4	3265.0	(734)
E	231.9	(52.13)	q_5	2389.0	(537)
F	401.7	(90.30)	q_6	876.3	(197)
G	231.9	(52.13)			

M = 9.02 MN · m (6.6510^6 ft-lbf)
V = 8.90 MN (2 x 10^3 lbf)

GP75-0131-108

FIGURE 36
TYPICAL END LOAD INTRODUCTION, CONCEPT 2

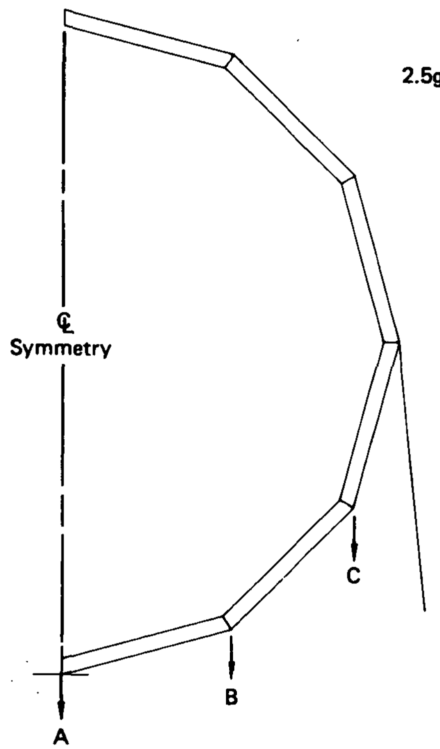

Vector	Magnitude	
	kN	(10^3 lbf)
A	44.0	9.89
B	66.4	14.92
C	24.5	5.52

GP75-0131-109

FIGURE 37
CONCEPT 2 TANK INERTIA LOADING

7.2.3 Detailed Analysis of Representative Components - Analysis of one of the tank-to-wing links is presented in Figure 38. In that analysis the CASD loads were identified and applied to the link. The link was then sized to carry the calculated load.

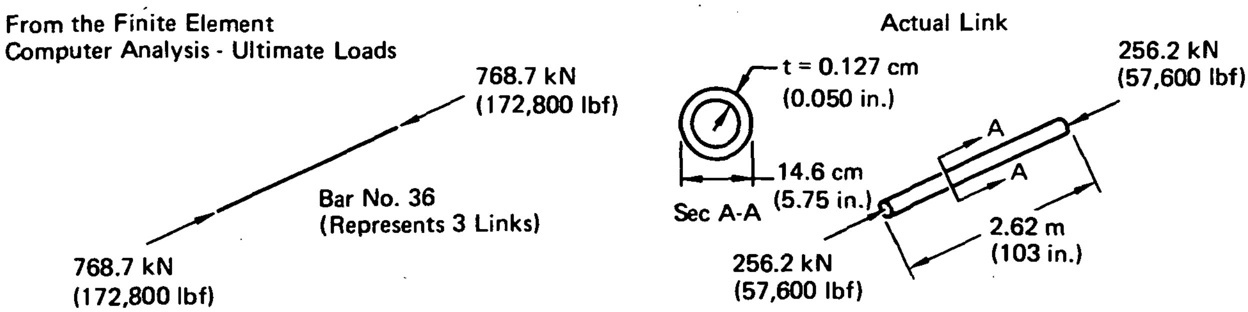

$$P_{cr} = \frac{\pi^2 E I}{L^2 A} = 273.48 \text{ kN } (61{,}480 \text{ lbf})$$

$$MS = \frac{273.48}{236.20} - 1 = +0.067$$

Tube Properties:
$A = 5.83 \text{ cm}^2$ (0.903 in.^2)
$I = 155.2 \text{ cm}^4$ (3.73 in.^4)
$\rho = 4.512 \text{ Mg/m}^3$ (0.163 lbm/in.^3)

Link Weight:
Tube: $A \times L \times \rho$ = 6.89 kg (15.2 lbm)
Endfitting: Estimated at = 1.36 kg (3.0 lbm) Constant
Total Link Weight = 9.62 kg (21.2 lbm)

GP75-0131-166

FIGURE 38
WING-TO-TANK LINK ANALYSIS, CONCEPT 2
Condition - 2.5g Flight

Actively cooled panels were analyzed in the same manner as for Concept 1. A typical analysis of an isogrid tank wall segment is also shown in Figure 39. Overall tank stability analysis showed this method of construction to be relatively insensitive to pressure stabilization. The resulting tank web thicknesses and equivalent weight thicknesses can be found in Figure 40 of Reference (1).

7.2.4 Structural Weight Refinement - As indicated in Figure 40, the estimated weight, based on statistical estimates for the integral tanks and Concept 1 experience, of the total center fuselage on Concept 2 was 3% low. The major reason for this discrepancy is the tank shell weight which is 2.27 Mg (5006 lbm) heavier than originally anticipated as a result of the integral stiffening requirements. This circumstance is mitigated, however, by the 1.46 Mg (3222 lbm) saving in longeron weight which was estimated solely on the basis of the Concept 1 aircraft.

2.5g Flight Condition

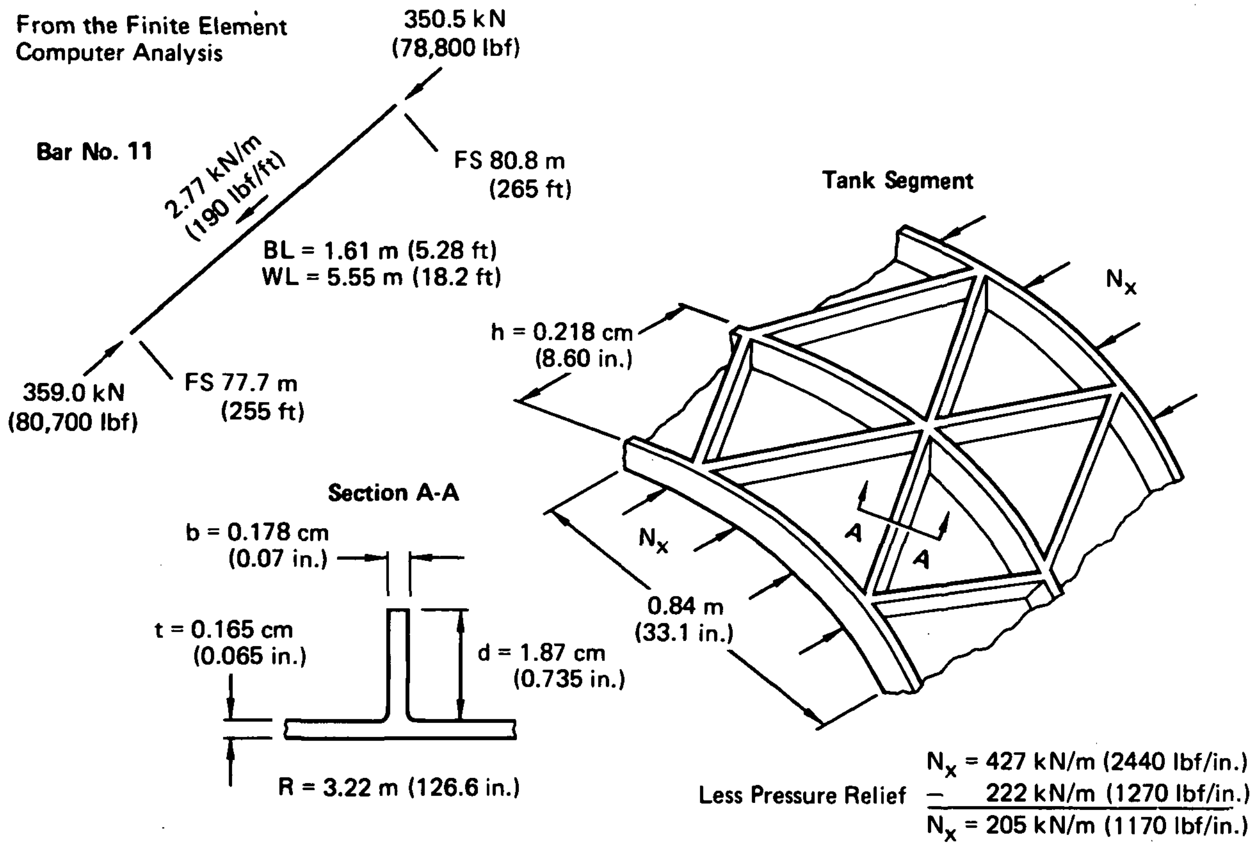

Using the Analysis Techniques of Reference 10: (Section 4.2)

$$\alpha = \frac{bd}{th} = 0.092$$

$$\delta = \frac{d}{t} 11.31$$

$$\beta = [3\alpha\,(1+\delta)^2 + (1+\alpha)\,(1+\alpha\delta^2)]^{1/2} = 7.47$$

$$t^* = t\,\frac{\beta}{1+\alpha} = 1.13 \text{ cm } (0.445 \text{ in.})$$

$$E^* = E\,\frac{(1+\alpha)^2}{\beta} = 13.21 \text{ GPa } (1.916 \times 10^6 \text{ psi})$$

$$\text{Margin of Safety} = \frac{208.4}{205} - 1 = +0.017$$

$$t_{eff} = t\,(1+\alpha) = 0.18 \text{ cm } (0.071 \text{ in.})$$

$$\bar{t} \text{ (Equivalent Weight Thickness)} = t\,(1+3\alpha) = 2.11 \text{ cm } (0.083 \text{ in.})$$

$$\text{Unit Weight} = \bar{t} \times \rho = 5.96 \text{ kg/m}^2 \ (1.22 \text{ lbm/ft}^2)$$

Temperature = 20.3 K (-423°F)
Material 2219-T87
ρ = 2.823 Mg/m^3 (0.102 lbm/in.^{3})

GP75-0131-225

FIGURE 39
TANK SHELL ELEMENT ANALYSIS, CONCEPT 2
Ultimate Loads Shown

Center Fuselage	Original Weight Estimate Mg (lbm)	Refined Weight Estimate from Detail Calculations Mg (lbm)	ΔO.W.E. Mg (lbm)
1. Actively Cooled Panels	8.90(19,625)	9.31 (20,540)	
2. Frames and Bulkheads	3.33(7,350)	2.89 (6,377)	
3. Longerons	2.18(4,800)	0.72 (1,578)	
4. Fuel Tanks	8.76(19,303)	11.03 (24,309)	
5. Tank Insulation	3.00 (6,619)	2.76 (6,076)	
6. Tank Supports	0.39(854)	0.80 (1,758)	
7. Misc Access Doors, Supports, etc.	2.46(5,425)	2.46 (5,425)	
Total	29.02(63,975)	29.97 (66,063)	+0.95 (+2,088)

GP75-0131-112

FIGURE 40
STRUCTURAL WEIGHT REFINEMENTS, CONCEPT 2

7.3 CONCEPT 3 WEIGHT REFINEMENT

The analytical process for structural weight refinement on the Concept 3 aircraft followed the same procedure previously established for Concepts 1 and 2. However, tank and fuselage structure were not separated as in the previous analyses. The decision had been previously made, as described in Section 6, to make the actively cooled fuselage covering completely nonstructural.

7.3.1 Finite Element Computer Model - The model used for analyzing the Concept 3 integral tanks is shown in Figure 41. On that illustration various elements of the structure such as a bulkhead, a tank frame, and the tank shell, are identified.

7.3.2 Input Loading Vectors - All of the input loading for the Concept 3 aircraft are quite similar to those identified for the previous concepts, except the frame loading. A typical frame load application is shown in Figure 42. The loads of Figures 14 and 15 were used to generate these inputs. The major difference is that the fuel and fuselage inertias are combined within a single basic substructure.

7.3.3 Detailed Analysis of Representative Components - An analysis of a representative stiffened tank shell is presented in Figure 43. This analysis is compatible with the one previously shown for Concept 2 in Figure 39. The resulting isogrid web thicknesses and equivalent weight thicknesses can be found in Figure 40 of Reference (1). A segment of one of the tank frames which doubles as part of the wing carrythrough is shown in Figure 44.

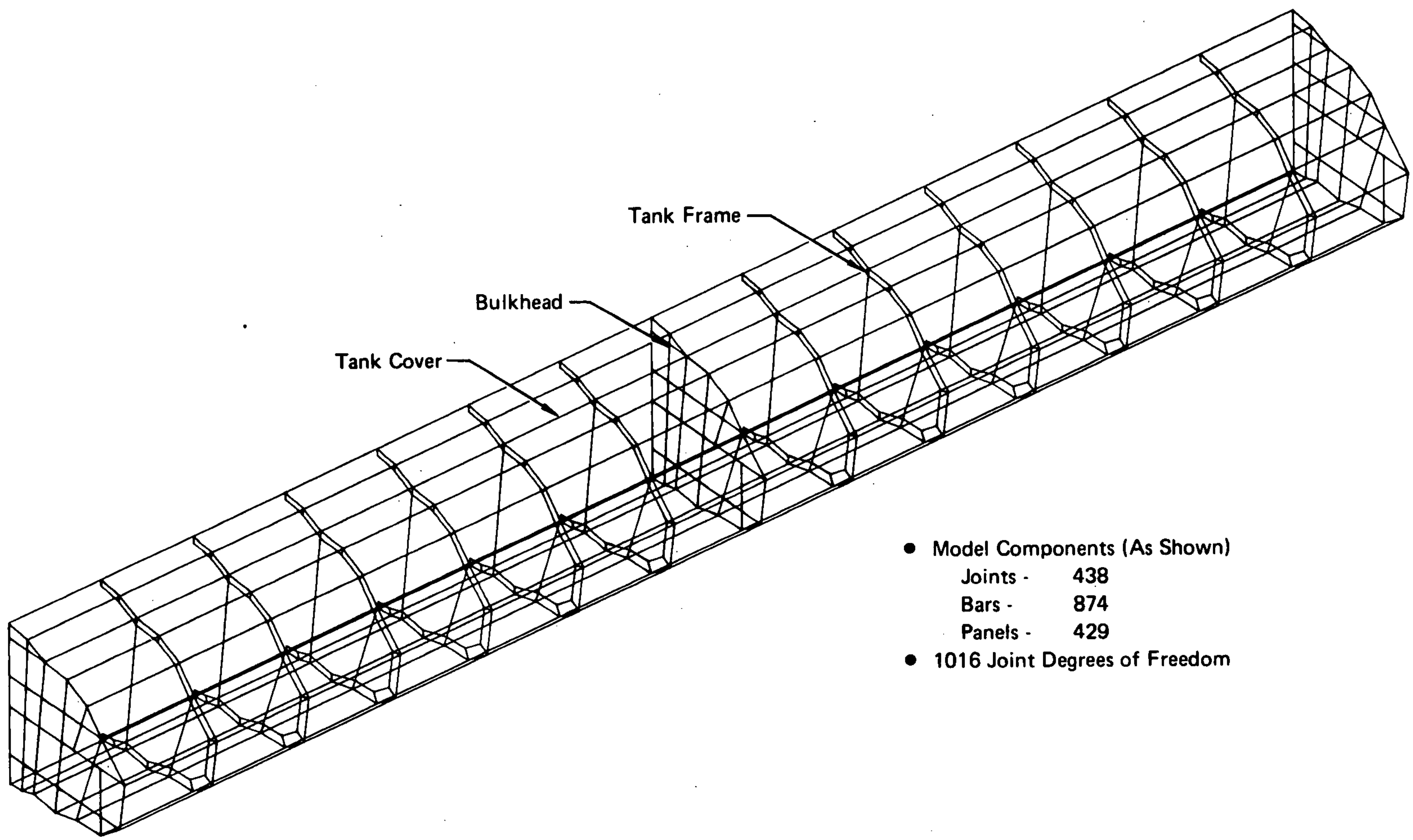

- Model Components (As Shown)
  - Joints - 438
  - Bars - 874
  - Panels - 429
- 1016 Joint Degrees of Freedom

FIGURE 41
CONCEPT 3 FINITE ELEMENT COMPUTER MODEL
Fuselage/Tank Area

GP75-0131-113

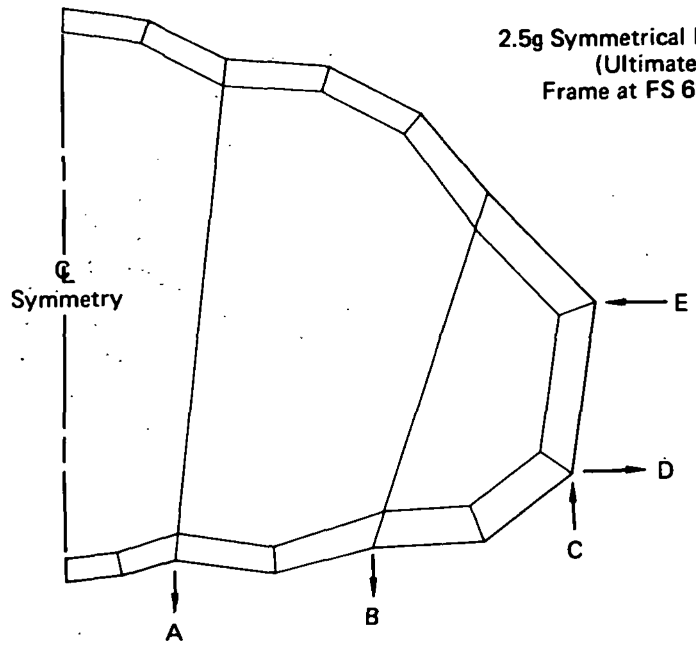

Vector	Magnitude	
	kN	(10^3 lbf)
A	122.6	27.57
B	101.3	22.77
C	353.8	79.54
D	1182.5	265.84
E	1182.5	265.84

GP75-0131-114

FIGURE 42
TYPICAL CONCEPT 3 FRAME LOADING

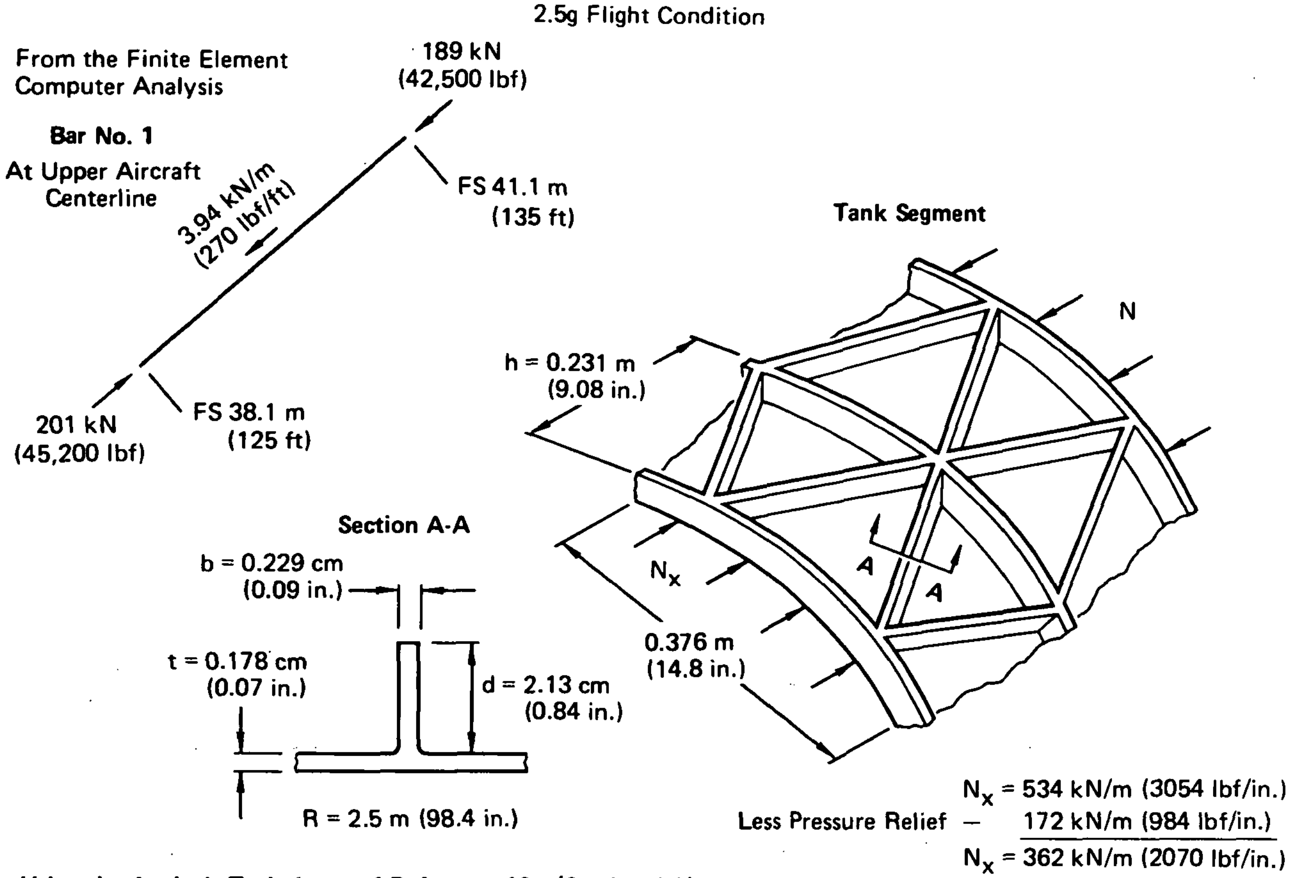

Using the Analysis Techniques of Reference 10: (Section 4.2)

$$\alpha = \frac{bd}{th} = 0.119$$

$$\delta = \frac{d}{t} = 12$$

$$\beta = [\,3\alpha\,(1+\delta)^2 + (1+\alpha)\,(1+\alpha\delta^2)]^{1/2} = 8.92$$

$$t^* = t\,\frac{\beta}{1+\alpha} = 1.36 \text{ cm } (0.537 \text{ in.})$$

$$E^* = E\,\frac{(1+\alpha)^2}{\beta} = 12.07 \text{ GPa } (1.75 \times 10^6 \text{ psi})$$

$$N_{c_r} = 0.397\, E^*\,(t^*)^2/R = 370.4 \text{ kN/m } (2115 \text{ lbf/in.})$$

$$\text{Margin of Safety} = \frac{370.4}{362} - 1 = +0.023$$

$$t_{eff} = t\,(1+\alpha) = 0.199 \text{ cm } (0.078 \text{ in.})$$

$\bar{t}$ (Equivalent Weight Thickness) $= t\,(1 + 3\alpha) = 0.242$ cm (0.095 in.)

Unit Weight $= \bar{t} \times \rho = 6.84$ kg/m^2 (1.40 lbm/ft^2)

Temperature = 20.3 K (–423°F)
Material 2219-T87
ρ = 2.823 Mg/m^3 (0.102 lbm/in.^{3})

GP75-0131-224

FIGURE 43
TANK SHELL ELEMENT ANALYSIS, CONCEPT 3
Ultimate Loads Shown

Frame at FS 64.9 m (213 ft)

2.5g Flight Condition
From the Finite Element Computer Analysis

Ultimate Loads

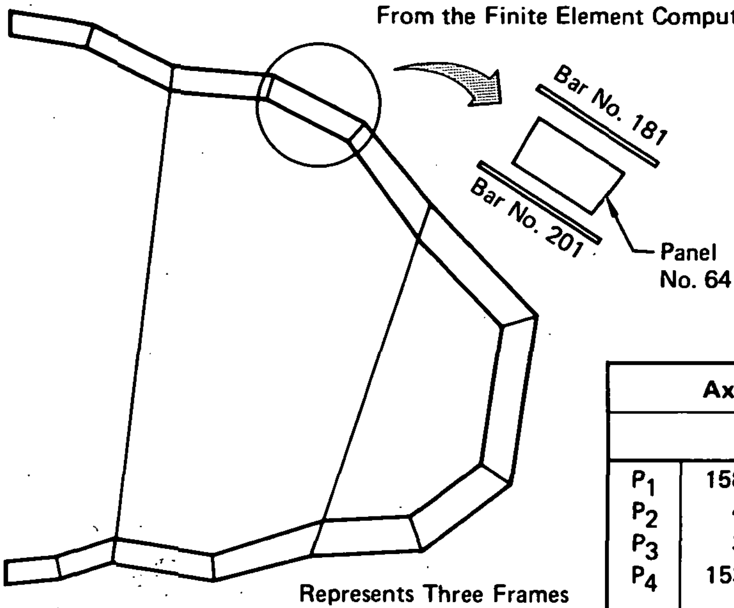

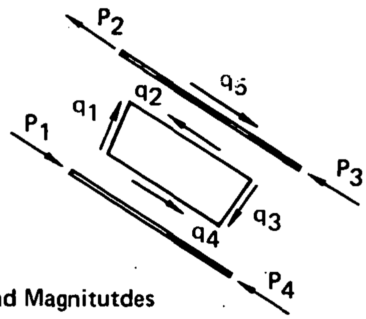

Load Magnitutdes

Axial Loads	kN	(10^3 lbf)	Shear Flows	kN/m	(lbf/in.)
P_1	1583.7	(356.0)	q_1	51.06	(291.6)
P_2	44.0	(10.0)	q_2	45.93	(262.2)
P_3	37.2	(8.3)	q_3	51.06	(291.6)
P_4	1537.8	(345.7)	q_4	56.79	(324.3)
			q_5	44.70	(255.3)

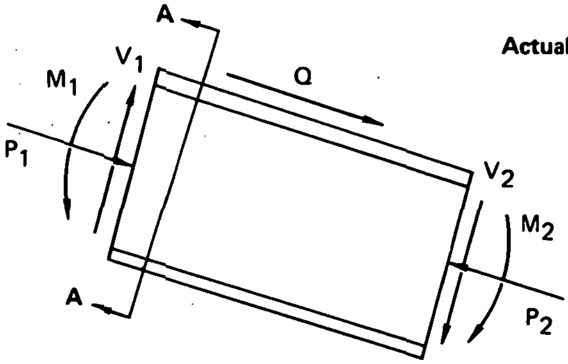

Actual Frame Segment

M_1 = 55.14 kN·m (488 x 10^3 in.-lbf)
P_1 = 513.1 kN (115.34 x 10^3 lbf)
V_1 = 3.46 kN (778 lbf)
Q = 13.40 kN (3013 lbf)
M_2 = 50.73 kN·m (449 x 10^3 in. - lbf)
P_2 = 524.9 kN (118 x 10^3 lbf)
V_2 = 3.46 kN (778 lbf)

Frame Cross Section

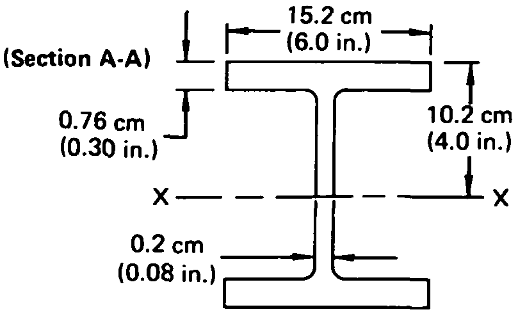

A = 2.71 mm^2 (4.2 $in.^2$)
$I_{x\text{-}x}$ = 23.4 μm^4 (56.1 $in.^4$)
ρ = 2.82 Mg/m^3 (0.102 $lbm/in.^3$)
Weight = 7.65 kg/m (0.43 lbm/in.)

Analysis of Section A-A

Bending Stress = $f_b = \frac{M_1 c}{I_{x\text{-}x}}$ = ±240.3 MPa (34,850 psi)

Axial Stress = $f_c = \frac{P_1}{A}$ = −109.3 MPa (−27,460 psi)

Maximum Tensile Stress = 51 MPa (7400 psi)
Margin of Safety is High

Maximum Compressive Stress = −429.6 MPa (62,300 psi)

Allowable Crippling Stress = −448.2 MPa (65,000 psi)

Margin of Safety = $\frac{-448.2}{-429.6} - 1$ = + 0.04

Shear Stress = $\frac{V_1}{th}$ = 8.48 MPa (1230 psi)

Margin of Safety is High

GP75-0131-116

FIGURE 44
TANK FRAME SEGMENT ANALYSIS, CONCEPT 3

7.3.4 <u>Structural Weight Refinement</u> - Figure 45 compares the original weight estimate, based on statistical estimates and the Concepts 1 and 2 experience, with the analytically refined weight of the Concept 3 fuselage/tank area. It is worthy of note here that although the tank weight is increased by almost 4.08 Mg (9000 lbm), there was enough weight saving in frames, bulkheads and the wing carrythrough to make the fuselage/tank area 2.26 Mg (4988 lbm) lighter than the original estimate. The accuracy of the original weight estimates for the fuselage/tank areas of all three concepts tends to lend credence to the estimated O.W.E.

	Original Weight Estimate Mg (lbm)	Refined Weight Estimate Mg (lbm)	Δ O.W.E. Mg (lbm)
Center Fuselage	31.39 (69,192)	32.26 (71,115)	+0.87 (+1,923)
1. Actively Cooled Panels	6.86 (15,133)	7.23 (15,929)	
2. Frames and Bulkheads	6.74 (14,357)	2.47 (5,445)	
3. Longerons	1.58 (3,479)	1.64 (3,620)	
4. Fuel Tanks	10.57 (23,292)	14.54 (32,047)	
5. Tank Insulation	3.00 (6,619)	3.11 (6,855)	
6. Tank Splice Links	0.76 (1,670)	1.30 (2,859)	
7. Misc Access Doors, Supports, etc	1.88 (4,142)	1.98 (4,360)	
Wing	22.61 (49,842)	19.68 (43,388)	−2.93 (−6,454)
Total	54.00 (119,034)	51.94 (114,503)	−2.06 (−4,531)

GP75-0131-117

FIGURE 45
STRUCTURAL WEIGHT REFINEMENTS, CONCEPT 3

8. FATIGUE, FRACTURE MECHANICS AND CREEP ANALYSIS

Part of the structural analysis of the aircraft evaluated the weight elements attributable to fatigue, fracture mechanics and creep requirements. Fatigue and fracture mechanics allowable stresses were developed as presented in Section 4. Creep allowables were established as discussed in Section 8.4.

The maximum range penalty resulting from fatigue requirements was 11.1 km (6 NM) for Concept 3. Fracture mechanics requirements resulted in a range penalty of 14.8 km (8 NM) which was for Concept 1 and creep analysis resulted in no range penalty to any of the aircraft.

8.1 EXPLANATION OF ANALYTICAL PROCESSES

Tension allowables appropriate to temperature and failure mode were defined for elements as the finite element models were being prepared for analysis. Since the computer would enlarge only those elements in which applied stresses exceeded allowables, it was relatively simple to identify those which were critical in tension. Fuel tank areas in which tank pressure would be added to tensile bending stresses were also identified. Minimum areas were rechecked in critical areas to assure that they were realistic. Then the change in weight of each tension critical element was assessed, if ultimate tensile strength was the design criteria.

8.2 FATIGUE CONSIDERATIONS

The fatigue analysis was based on the load factor spectrum presented in Figure 7. Tank pressurization effects were added for the cryogenic tank analyses. Miner's rule cumulative damage analyses were conducted to determine the allowable design limit stresses presented in Section 4. S-N curves for fatigue analysis at elevated and cryogenic temperature were taken from References (12) and (13), respectively. The effects of fatigue analysis on weight and range of the study aircraft are as follows:

Concept 1:

Fuselage Covering - Fatigue allowable stress is greater than ultimate tensile stress divided by the factor of safety of 1.5. No weight was added to the fuselage covering for fatigue.

LH_2 Tank - The tank was designed by burst pressure and exhibits positive margins of safety in both the parent metal and in the weld joint. No weight was added for fatigue.

Concept 2

a. Fuselage Covering - The "semistructural" center fuselage cover works to a limit stress of only 55.2 MPa (8000 psi) and is not critical in fatigue. No weight added.

b. LH_2 Tank - Eight limited areas in the tank frames were identified as being critical in fatigue. A total of only 20.4 kg (45 lbm) of material was required to reduce the stresses in these areas below the fatigue allowable stress. This resulted in a range penalty of less than 1.9 km (1 NM.) The K_T used for consideration was 3.06.

Concept 3:

Fuselage Covering - Consists of completely non-structural actively cooled panels. No fatigue penalty.

LH_2 Tank - Limited areas in several of the aft tank frames were found to require added area to limit the applied stress to the fatigue allowables. The 213 kg (470 lbm) of aluminum added for this purpose is equivalent to a range loss of approximately 11.1 km (6 NM.) K_T used for analysis was 3.06.

8.3 FRACTURE MECHANICS CONSIDERATIONS

Fracture Mechanics (Crack Growth) analysis utilized the same type of cumulative damage analysis and the same spectrum as was used in the fatigue analysis. Fuselage covering analysis was compatible with the Actively Cooled Panel Program, Reference (8), and considered a 0.127 mm (0.005 in) crack growing from a fastener hole. Allowable stresses were based on the number of flight hours required for the crack to grow to critical length. Allowable stresses in the cryogenic tank analysis, however, were based on defects with less than a 98% probability of being detected. Those defects were a surface scratch on the parent material or a 0.25 mm x 6.35 mm (0.01 in x 0.025 in) flaw in the weld. The flaws were not allowed to grow through the local material thickness within the specified 10,000 hour design service life between scheduled inspections. Crack growth data for elevated temperature were taken from Reference (14) and for cryogenic analysis from Reference (15). The effects of crack growth analysis on weight and range of the study aircraft are presented below:

Concept 1:

Fuselage Covering - Reduced allowables to prevent critical crack growth in the actively cooled panels required addition of 268 kg (590 lbm) of material. This is equivalent to a change in range of 14.8 km (9 NM.)

LH_2 Tank - The tank is designed by ultimate burst pressure and exhibits positive margins of safety for fracture mechanics allowables both in the parent material and the weld joint. No weight was added.

Concept 2:

Fuselage Covering - Applied stresses are well below the fracture mechanics allowables. No weight added.

LH_2 Tank - No applied stresses were found to be above the crack growth allowables. No weight added.

Concept 3:

Fuselage Covering - Nonstructural actively cooled panels. No weight added.

LH_2 Tank - No applied stresses were found to be above the crack growth allowables. No weight added.

8.4 CREEP ANALYSIS

A creep analysis was conducted on the 2219-T87 aluminum alloy selected for use in the study aircraft. As anticipated, no weight was added to any of the aircraft concepts for creep considerations.

The structural design criteria presented earlier in this report specify that "Creep Analysis" shall show 0.5% or less creep in the design service life of the aircraft. Creep and creep rupture properties for 2219-T87 aluminum alloys were taken from Reference (14). This data was reduced into a curve showing life versus applied stress level (for 0.5% creep) by using the Larsen Miller parameter, which is explained more fully in Reference (15). This curve is presented as Figure 46. It represents a constant temperature of 394 K (250°F).

The time to be spent at various stress levels is extremely difficult to correlate with the fatigue spectrum presented as a part of the structural design criteria. Three conservative assumptions were made: (1) to divide the fatigue spectrum upper limits into three segments according to the upper limit load factor; (2) to proportion the total aircraft service life

(10,000 flight hours) according to the cumulative number of loading cycles in a segment; and (3) to assume that the aircraft spent the entire time at the upper limit stress for a given segment. It was further assumed that the cryogenic fatigue allowable of 262 MPa (38,000 psi) was applied at 394 K (250°F) and was a limit stress corresponding to a load factor of 2.5.

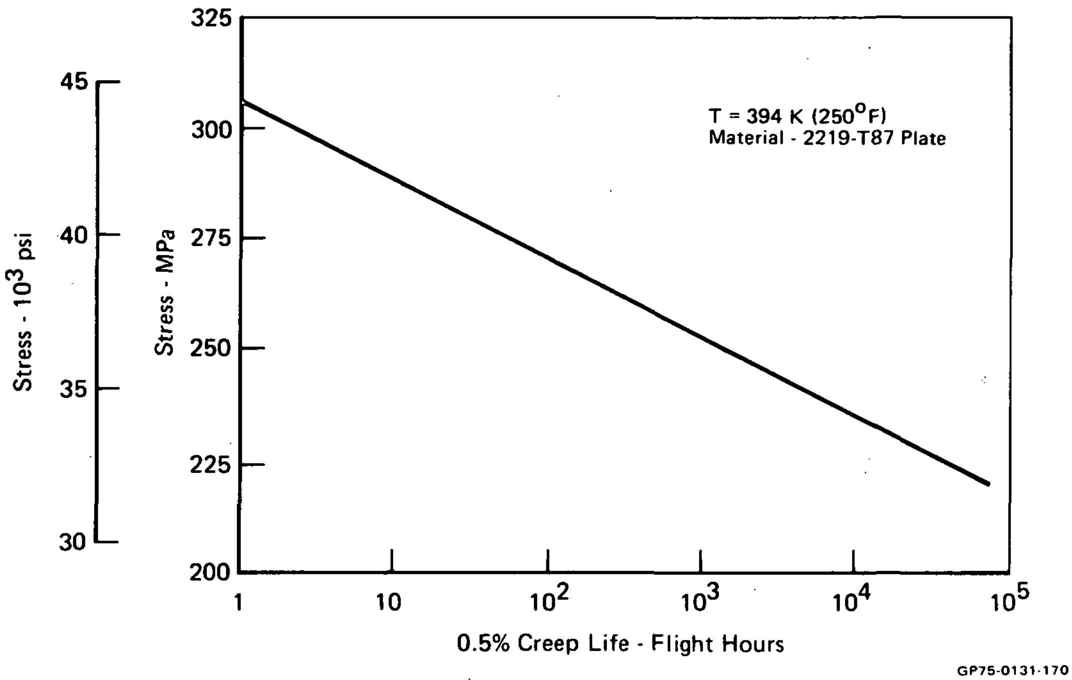

FIGURE 46
APPLIED STRESS vs LIFE FOR 0.5% CREEP

The three service life segments thus derived were: (a) a 9999 hour life at 2.0g (limit stress = 210 MPa (30.4 psi)); (b) a 0.955 hour life at 2.5g (limit stress = 262 MPa (38.0 psi)); and (c) a 0.045 hour life at 2.9g (limit stress = 304 MPa (44.1 psi)). The analysis and its results are presented in Figure 47. Even with the extraordinarily conservative assumptions discussed above, only 0.23% creep would be experienced. It was concluded then that creep was not a problem to be further considered for this study.

Time Increment	Stress MN/m^2 (10^3 psi)	N - Life (For 0.5% Creep) (hr)	n - Exposure (hr)	Damage, n/N (percent)
1	210 (30.4)	23,200	9,999	0.431
2	262 (38.0)	300	0.955	0.003
3	304 (44.1)	1.4	0.045	0.032
				Σ = 0.466

T = 394 K (250°F)
Total Creep = 0.5 x 0.466 = 0.23%

GP75-0131-119

FIGURE 47
CUMULATIVE CREEP ANALYSIS

9. CONCLUSIONS AND RECOMMENDED AREAS FOR FUTURE INVESTIGATION

Several conclusions were drawn from the structural analysis and interdisciplinary work involved in synthesis of the three study aircraft. These conclusions form a basis for recommendation of future studies in the area of actively cooled hypersonic cruise vehicles.

9.1 CONCLUSIONS

a. Integral Tank Design - Integrally machined stiffening of the tank walls while providing the most weight efficient use of materials, results in higher production costs. Alternate methods of stabilizing the tank walls are available which will reduce production cost, however such methods generally result in increased weight and reduced range. Monocoque tank walls (the heaviest of all alternates examined) were found, as reported in Reference (1), to reduce the producibility cost factor for Concept 3 from 3.0 to 1.8 and are judged worthy of consideration for operational systems.

b. Fatigue and Fracture Mechanics - It was anticipated that fatigue and fracture mechanics requirements would have a dramatic impact on the weight of the study aircraft. To the contrary the effect was small. It is concluded that the reason for this is the large size of the aircraft which leads to low working stresses, even when minimum gages are used for construction.

c. Accommodation of Thermal Deflections - The need for thermal strain relief was brought about by the large temperature differential, 346K (623°F), between the actively cooled structure and the cryogenic tanks, which are insulated externally. Without relief the resulting thermal stresses would be above yield strength. Internal tank insulation, which would have reduced or eliminated the temperature differential, was found to be non-competitive with externally applied insulation in terms of aircraft range as discussed in Reference (2). The primary reason for that effect was permeation of the internal insulation by gaseous hydrogen. Producibility analysis, presented in Reference (1), shows that the systems utilized for accommodation of thermal deflection in the integral fuel tank aircraft are major contributors to their relative cost disadvantage. Significant savings in relative production cost could be accomplished if vapor barrier insulation systems were available for incorporation inside the tank walls thus eliminating the need for accommodation of thermal strains.

d. Non-Integral Tank Design - Aircraft size and magnitude of the internal pressure are significant factors. If the aircraft and tanks were smaller or the tank proportions were altered the probability is that the most weight efficient material usage would require the use of integral stiffening. A similar effect would result if tank pressures were reduced as a result of using sub-cooled hydrogen in lieu of normal boiling point hydrogen. Thus, a trade would have to be made to evaluate the benefit that the reduced weight integral stiffening provides against the added aircraft cost.

e. Purge Pressure - Accommodation of the 3.45 kPa (0.5 psi) purge pressure had negligible effect on aircraft performance.

f. Fuel Tank Design Conditions - The Concept 1 monolithic non-integral fuel tanks were designed to burst pressure requirements and were not limited by fatigue or fracture mechanics requirements. The Concept 2 and 3 tank frames, however, were critical at the tank frames for fatigue design as noted in Section 7. It was determined, then, that more inherent reliability could be found in the Concept 1 non-integral tanks which were also shown to be lower in cost and more readily maintained than the integral tank concepts.

9.2 RECOMMENDED AREAS FOR FUTURE INVESTIGATION

a. Integral Tank Design - Accommodation of thermal strains and integrally machined stiffening concepts for the tank walls are the major contributors to the high relative costs of integral tankage, as discussed in Reference (1). A new series of designs could be initiated with the advent of a viable hydrogen vapor barrier. The barrier against gaseous hydrogen leakage would allow the practical use of insulation on the inside of the tank wall and, thereby, reduce or eliminate the temperature differential between the tank wall and actively cooled structure. It is possible that the honeycomb construction active cooling concept and load carrying tank wall could be combined in such a manner that the honeycomb would provide the required stiffening and large structural thermal deflections would no longer exist and volumetric efficiency would be enhanced. It is therefore recommended that a study be conducted to determine the effect of utilizing a vapor barrier system on a circular tank design similar to that of Concept 2.

b. Non-Integral Tank Design - The effect of tank size proportion and design pressures was a dominant factor in design of the Concept 1 non-integral tanks. Use of sub-cooled (or slush) hydrogen would allow use of lower tank pressurization and also reduce the amount of boil-off fuel lost during the mission. Reference (16) concluded that the use of sub-cooled hydrogen is feasible and economical. It is recommended that a further study be conducted to evaluate the performance and cost effects of the use of sub-cooled hydrogen on both the Concept 1 and Concept 2 study aircraft. Concept 2 would be included for comparison.

c. Materials - There is currently large interest in the use of cryogenic hydrogen as an energy conservation measure. Practical construction of tankage for this fuel will depend on extensive new knowledge of material properties specifically suited for this purpose. It is therefore recommended that a study be conducted to determine fully the design allowables for cryogenic construction materials.

10. REFERENCES

1. NASA CR-132668, "A Fuselage/Tank Structure Study for Actively Cooled Hypersonic Cruise Vehicles - Aircraft Design Evaluation," T. Nobe, 30 June 1975.
2. NASA CR-132669, "A Fuselage/Tank Structure Study for Actively Cooled Hypersonic Cruise Vehicles - Active Cooling System Analysis," J. E. Stone, 30 June 1975.
3. NASA Request for Proposal 1-08-4129, "A Fuselage/Tank Structure Study for Actively Cooled Hypersonic Cruise Vehicles," Exhibit A, 17 August 1973.
4. Federal Aviation Regulations, Volume III, Part 25 Airworthiness Standards: Transport Category Airplanes.
5. NASA SP-8057, "Structural Design Criteria Applicable to a Space Shuttle," January 1971, Revised March 1972.
6. NASA CR-XXXX, "A Fuselage/Tank Structure Study for Actively Cooled Hypersonic Cruise Vehicles - Summary," C. J. Pirrello, 30 June 1975.
7. Military Specification Mil-A-008860A (USAF), "Airplane Strength and Rigidity, General Specification for", 31 March 1971.
8. NASA Contract No. NAS-1-12919, "Design and Fabrication of an Actively Cooled Panel", 1974.
9. NASA CR 124075, "Isogrid Design Handbook", McDonnell Douglas Astronautics Company, February 1973
10. Military Handbook Mil-HDBK-23A, "Structural Sandwich Composites", 30 December 1968.
11. "Analysis and Design of Flight Vehicle Structures", E. F. Bruhn.
12. AFML-TDR-64-280, "Cryogenic Materials Handbook, Volumes I and II", F. R. Schwartzberry.
13. Alcoa Research Laboratory Report ARL 9-68-23.
14. Report MDC G2654, "Mechanisms of Fatigue Crack Propagation in 2219-T87 Aluminum in Argon and 3.5% NaCI Solution Environments", McDonnell Douglas Corporation, August 1972.
15. NASA-CR-115388, "Determination of Design Allowable Properties - Fracture of 2219-T87 Aluminum Alloy", the Boeing Company.
16. NASA CR-114326, "Hypersonic Research Facilities Study, Volume III, Part 2", October 1970.